Science of the Total Environment 729 (2020) 138443

Contents lists available at ScienceDirect

Science of the Total Environment

journal homepage: www.elsevier.com/locate/scitotenv

# Water quality impacts of urban and non-urban arid-land runoff on the Rio Grande

Peter J. Regier[a,*], Ricardo González-Pinzón[a], David J. Van Horn[b], Justin K. Reale[c], Justin Nichols[a], Aashish Khandewal[a]

[a] Department of Civil, Construction & Environmental Engineering, University of New Mexico, Albuquerque, NM 87131, USA
[b] Department of Biology, University of New Mexico, Albuquerque 87131, USA
[c] U.S. Army Corps of Engineers, Albuquerque District, Albuquerque 87109, USA

## HIGHLIGHTS

- Urban stormwater quality in arid regions is poorly understood.
- We compared urban and non-urban runoff quality dynamics in an arid region.
- Physicochemical factors are linked to non-urban runoff dynamics.
- Biogeochemistry processes are linked to urban runoff dynamics
- Urban and non-urban storm runoff pose ecological and management concerns.

## GRAPHICAL ABSTRACT

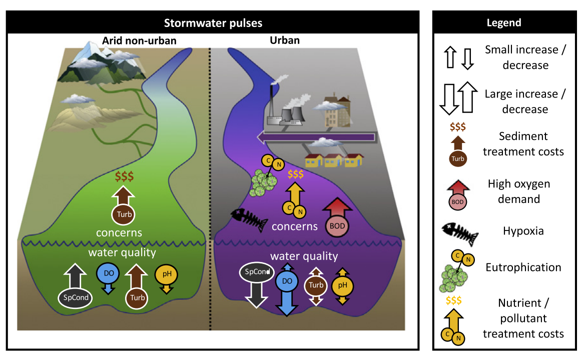


## ARTICLE INFO

*Article history:*
Received 19 November 2019
Received in revised form 30 March 2020
Accepted 2 April 2020
Available online 24 April 2020

Editor: Sergi Sabater

*Keywords:*
High frequency monitoring
Urban and non-urban runoff
Hypoxia
River ecology
Arid regions

## ABSTRACT

Urban surface runoff from storms impacts the water quality dynamics of downstream ecosystems. While these effects are well-documented in mesic regions, they are not well constrained for arid watersheds, which sustain longer dry periods, receive intense but short-lived storms, and where stormwater drainage networks are generally isolated from sewage systems. We used a network of high-frequency in situ water quality sensors located along the Middle Rio Grande to determine surface runoff origins during storms and track rapid changes in physical, chemical, and biological components of water quality. Specific conductivity (SpCond) patterns were a reliable indicator of source, distinguishing between runoff events originating primarily in urban (SpCond sags) or non-urban (SpCond spikes) catchments. Urban events were characterized by high fluorescent dissolved organic matter (fDOM), low dissolved oxygen (including short-lived hypoxia <2 mg/L), smaller increases in turbidity and varied pH response. In contrast, non-urban events showed large turbidity spikes, smaller dissolved oxygen sags, and consistent pH sags. Principal component analysis distinguished urban and non-urban events by dividing physical and biogeochemical water quality parameters, and modeling of DO along the same reach demonstrated consistently higher oxygen demand for an urban event compared to a non-urban event. Based on our analysis, urban runoff poses more potential ecological harm, while non-urban runoff poses a larger problem for drinking

* Corresponding author.
*E-mail address:* pregier@unm.edu (P.J. Regier).

https://doi.org/10.1016/j.scitotenv.2020.138443

water treatment. The comparison of our results to other reports of urban stormwater quality suggest that water quality responses to storm events in urban landscapes are consistent across a range of regional climates.


## 1. Introduction

Precipitation events affect water quality by discharging runoff with distinct physical, chemical, and biological characteristics to receiving waters. Surface stormwater runoff from urban and non-urban landscapes has been linked to increased suspended sediments (Freeman and Schorr, 2004), altered temperature regimes (Herb et al., 2008), mobilization of nutrients and pollutants (Li et al., 2015; Raymond and Saiers, 2010), changes in nutrient limitation (Yang and Toor, 2018), and lower dissolved oxygen levels (Dahm et al., 2015; Mallin et al., 2009; Reale et al., 2015). In turn, changes in water quality can degrade downstream aquatic ecosystems through nutrient-driven eutrophication (Fenn et al., 1998), ecotoxicity from mobilization of metals and other contaminants (Brix et al., 2010; Galfi et al., 2017; Rice et al., 2018), higher fecal bacteria counts (Mallin et al., 2009; Fluke et al., 2019), the spread of diseases (Jofre et al., 2010), spread of antibiotic resistance (Almakki et al., 2019), and increased oxygen demand associated with hypoxia (Mallin et al., 2006). Such negative impacts represent a threat to drinking water security, the health of aquatic flora and fauna, and a growing and evolving challenge for water managers and regulators.

To successfully address water quality concerns associated with urban and non-urban surface stormwater runoff, it is essential to understand the complex linkages between runoff quality and watershed characteristics, including hydrology, lithology, biogeochemistry and, perhaps most significantly, anthropogenic modification (Chadwick et al., 2006; Lintern et al., 2018). Increased urbanization is associated with changes in stormwater timing, quantity and quality, including increased hydrograph peaks and runoff volumes (Miller and Hess, 2017; Zeiger and Hubbart, 2018), and a distinct cocktail of anthropogenic chemicals mobilized by runoff (Kaushal et al., 2018). These intermittent pulses of chemicals shift the quality and quantity of carbon and nutrients (Hosen et al., 2014; Ding et al., 2015) and alter biogeochemical and microbial conditions (Chadwick et al., 2006; Rivers et al., 2018).

An increased research focus on understanding the behavior and drivers of urban streams has uncovered general commonalities in the effects of catchment development on runoff characteristics, but continues to prompt important and unanswered research questions about mechanisms driving urban runoff quantity and quality (Booth et al., 2016; Wenger et al., 2009; Hopkins et al., 2015). Historically, urban runoff research has focused primarily on mesic systems, where widespread urbanization, higher annual rainfall and regular storms yield frequent urban runoff events. In contrast, urban runoff in arid and semi-arid regions, which account for 40% of global land area (Feng and Fu, 2013), is comparatively understudied (Jefferson et al., 2017; Kingsford, 2006). In the Southwest United States, the North American monsoon season accounts for a large percentage of annual precipitation, characterized by high-intensity, short-lived storms that vary in frequency from daily to intermittent (Adams and Comrie, 1997; Sheppard et al., 2002). Large, intense rain events following extended dry periods have considerable potential to be biogeochemically significant for receiving waters. For example, in a semi-arid catchment, Brooks et al. (2007) found that monsoon storms accounted for 96% and 97% of annual carbon and nitrogen fluxes, respectively. Likewise, Wise et al. (2019) reported that a single storm lasting just hours flushed organic carbon loads from a semi-arid urban catchment that were equivalent to 5 days of baseflow loads. However, capturing these events is logistically challenging (Vivoni et al., 2006), and has resulted in a gap in our understanding of stormwater runoff processes and management in arid watersheds (Gautam et al., 2010; Jefferson et al., 2017).

The Rio Grande is the fifth longest river in North America, with a watershed covering portions of seven states in two countries (Fig. 1). The Middle Rio Grande (MRG) spans a semi-arid/arid reach in New Mexico, USA, between Cochiti to Elephant Butte reservoirs that is increasingly impacted by urbanization, primarily from development in and around the Albuquerque metropolitan area. Monsoon-driven, localized urban runoff enters the MRG in the summer during periods of low baseflow. Because summer flows in the MRG at Albuquerque are often low (Archdeacon, 2016), and the volume of runoff flushed from the largely impervious urban catchment can be very high, urban inputs can comprise the majority of Rio Grande discharge during medium or large storm events. This raises concerns about impacts of urban runoff on water quality and downstream ecosystem health in the MRG. In 2018, the year of this study, the United States Geological Survey (USGS) stream gauge on the Rio Grande at Embudo (#08279500) recorded the lowest discharge in a century on the Rio Grande (June 23, 2018: 3.88 $m^3/s$, 1889–2018 average: 24.9 $m^3/s$). In the MRG, the USGS gauge at Central (#08330000; Fig. 1) recorded the lowest mean annual discharge for 2018 (11.2 $m^3/s$) since 1977. Coupled with an above-average monsoon season in terms of total precipitation (measured at the USGS North Floodway Channel gauge #08329900), the climatic conditions in 2018 match climate change predictions for the MRG. These forecasts predict reduced snowpack (driving lower annual discharge in the snowpack-driven rivers of the Western United States), and changes in the intensity and frequency of precipitation regimes (Blythe and Schmidt, 2018; Chavarria and Gutzler, 2018; Dettinger et al., 2016). As such, urban runoff conditions during the 2018 monsoon season may represent the predicted new normal for urban stormwater contributions to large aridland rivers.

In this study we captured surface stormwater runoff water quality dynamics using high-frequency water quality data collected throughout the summer and fall of 2018 by situ sensors located along the MRG, which spans a gradient of urbanization. Storm events originating from primarily non-urban and primarily urban watersheds were identified. We note that urban runoff is sourced from drainage networks separate from sewage networks (i.e., stormwater does not mix with sewage). We compared urban and non-urban storms to 1) investigate differences in water quality signatures and relationships to catchment hydrology, 2) assess potential drivers, 3) identify potential ecological and management implications for receiving waters and 4) contextualize our findings within the broader urban stormwater literature.

## 2. Methods

### 2.1. Site description

Modeling tools available at modelmywatershed.org (Stroud Water Research Center, 2020) were used to calculate land cover, land use, and stream order statistics. Catchment areas were collected from USGS gauges (#08328950, #08329900). Annual precipitation in this reach is largely dominated by summer rain events associated with the North American Monsoon. Total precipitation measured at the NDC USGS gauge near Alameda (#08329900) for the 2018 monsoon season (June–October) was above average for 2000–2018, and accounted for almost 80% of 2018 annual rainfall. Water quality data for this study were collected along a reach of the MRG, across a gradient of land-use, from primarily non-urban to primarily urban (Fig. 1). The most upstream monitoring site is directly downstream of the Cochiti Dam spillway (USGS gauge #08317400). The next downstream monitoring site is at the US 550 Bridge in Bernalillo (B550, located ~42 km downstream of

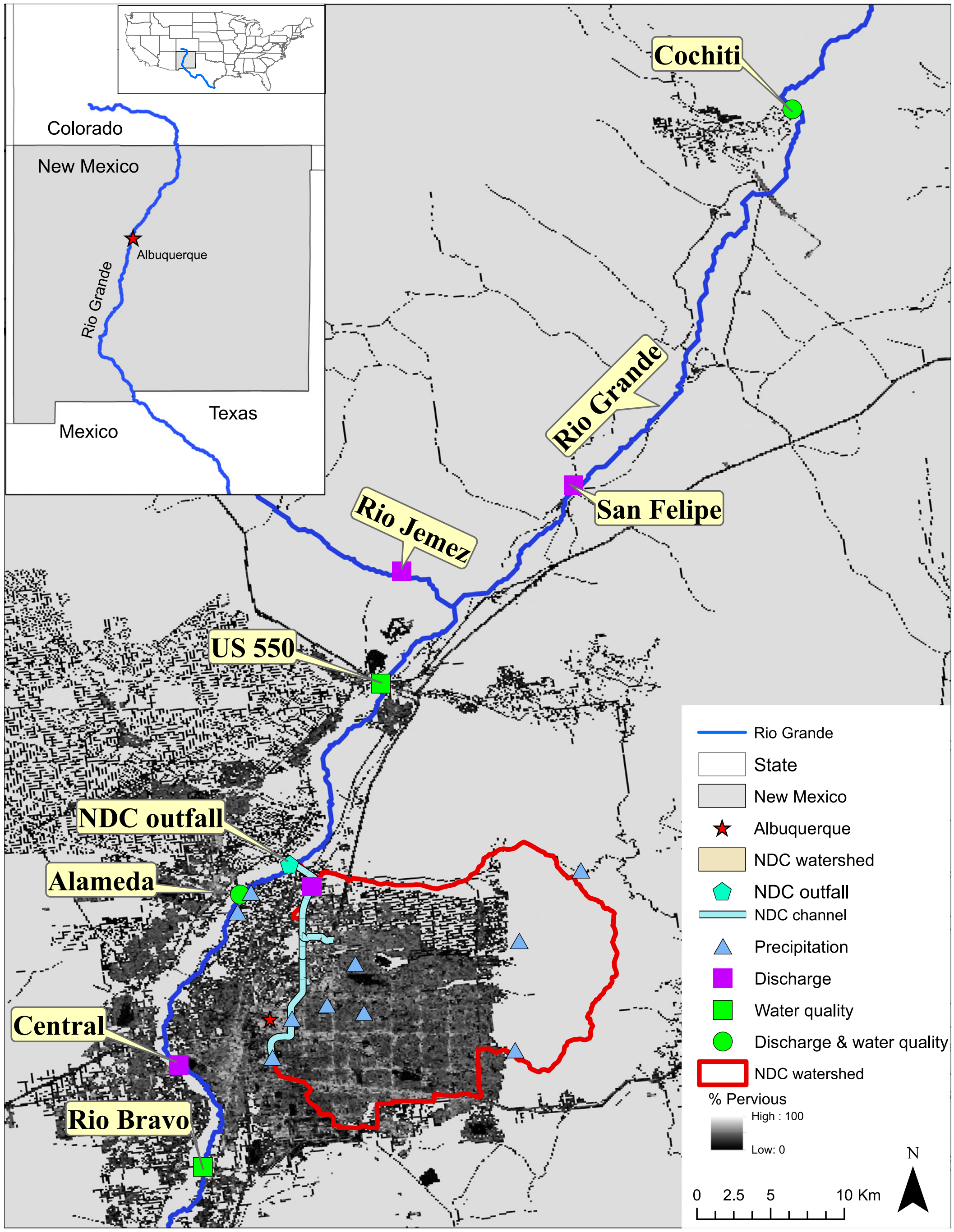


**Fig. 1.** Site map of the study reach along the Middle Rio Grande. Sondes are located at Cochiti, US 550 (B550 in text), Alameda, and Rio Bravo. Grayscale shading indicates level of impervious land cover, which is largely concentrated in the highly developed North Diversion Channel watershed near Albuquerque.

Cochiti). This site is located below the confluence of the Jemez River with the Rio Grande. The Jemez River drains a 2678 $km^2$ watershed comprised of 1st-5th order streams across forested montane, high elevations areas and low elevation arid scrub-land, with minimal agricultural influence (~1% of stream length effected), and limited (<1%) developed land. In addition to the Jemez River, the reach of the Rio Grande between Cochiti and B550 receives ephemeral inflows from a variety of smaller watersheds which drain largely undeveloped lands (average 3% developed land by area). The third monitoring site, Alameda, is located ~61 km below Cochiti Dam and marks a sharp transition in land-use and land cover (Fig. 1). Notably, this site is immediately downstream of the outfall of the North Diversion Channel (NDC, drainage area of 228 $km^2$), which drains a combination of developed (~45%) and undeveloped areas (including federally managed forest and other open space) in the Albuquerque Metropolitan Area. The NDC is a network of ephemeral, concrete-lined stormwater drainage channels and flows primarily during and immediately after storm events (~75 days a year on average, Storms et al., 2015). The stormwater drainage system only drains surface runoff and is independent of the sewer system. During monsoon storms, ~85% of all urban stormwater originating in Albuquerque moves as surface runoff into the NDC and ultimately drains into the Rio Grande (Storms et al., 2015). In addition, several ungauged arroyos and other smaller stormwater conveyance structures discharge into the Rio Grande upstream and downstream of the Alameda monitoring station (Storms et al., 2015). The study reach is bounded downstream by the Rio Bravo monitoring station (~83 km below Cochiti), which receives additional discharge from multiple ungauged inputs during storm events. Precipitation frequencies provide useful information about which regions of a watershed may contribute more or less rainfall to a given runoff event, and we selected several sites to characterize rainfall differences across the landscape using NOAA precipitation frequency estimates (https://hdsc.nws.noaa.gov/hdsc/pfds/pfds_map_cont.html). The highest precipitation depths for a 2-h event at a 5-year recurrence interval were from the headwaters of the Jemez River (43.4 mm), followed by the lower Jemez River watershed (37.1 mm), the NDC watershed (34.3 mm), and finally adjacent to the Rio Grande (31.7 mm), following a gradient of elevation consistent with orographic control (Sheppard et al., 2002).

### 2.2. Data collection

Discharge measurements were obtained at 15-min resolution from USGS stream gauges including the Jemez River downstream of Jemez Canyon Dam (#08328950), the NDC outfall (#08329900), and the Rio Grande near Alameda (#08329918). Precipitation data were collected throughout the NDC watershed from multiple USGS gauges (#08329900, #350554106283230, #350954106282330, #351057106384330, #351140106381230, #351229106260830, #08329700, #08329835, #08329838, #08329840, #08329880). Here, we report precipitation as the average of all gauges to provide a spatially representative approximation of rainfall across the NDC watershed. All USGS data were imported and formatted using the *dataRetrieval* package (Hirsch and De Cicco, 2015) in R (R Core Team, 2018).

Water chemistry data were collected using multiple high-frequency in-situ instruments (Fig. 1). Data for temperature (°C), specific conductivity (SpCond; μS/cm), dissolved oxygen (DO; mg/L), pH, and turbidity (FNU) were collected at 15-min intervals at the B550, Alameda, and Rio Bravo monitoring sites (Fig. 1) using EXO2 water quality sondes (YSI, Yellow Springs, OH), except at Cochiti where an In Situ Troll 600 is deployed and maintained by the USGS. Sondes were serviced and checked for calibration drift approximately every three weeks following USGS standard operating procedures (Wagner et al., 2006). All YSI sondes were equipped with wipers to minimize fouling of sensor heads. The sonde deployed at Alameda was also equipped with a fluorescent dissolved organic matter (fDOM) sensor, calibrated to report quinine sulfate units (QSU). Corrections for fDOM were conducted following procedures in the literature (Downing et al., 2012) for temperature and turbidity. Temperature corrections match previous reports for similar sensors (e.g. Watras et al., 2011; Regier and Jaffé, 2016). Details regarding correction of fDOM data are described in detail in the Supplemental Information, including an expanded correction for suspended sediment interference in fDOM measurements in highly turbid systems (Fig. S1). Nitrate and UV absorbance at 254 nm ($A_{254}$) values were measured at Alameda using a SUNA V2 optical nitrate sensor (Sea-Bird Scientific, Bellevue, WA). We note that $A_{254}$ measurements represent absorbance, which is unitless, and do not account for differences in pathlengths between instruments. While Hu et al. (2002) recommend reporting absorption coefficients ($a_{254}$, $m^{-1}$), calculated following Eq. (2) in Kowalczuk et al. (2010), recent papers reporting UV absorbance values in relation to sensors have reported $A_{254}$ values. As such, we report both $A_{254}$ and $a_{254}$ values in Fig. S5. Grab samples were collected at Alameda using an ISCO auto-sampler (Teledyne) to calibrate the fDOM:DOC and turbidity:total suspended solids (TSS) relationships during portions of three storm events (August 9 for DOC samples, August 15 and 22 for TSS samples). DOC samples were analyzed at the North Carolina State University Aquatic Biogeochemistry laboratory using an OI 1030 TOC analyzer using wet chemical oxidation mode and calibrated to caffeine standards ranging from 0 to 20 mg C $L^{-1}$. TSS were measured as change in dry weight after filtration of a known volume using pre-combusted, pre-weighed 0.7 μm GF/F filters.

### 2.3. Defining urban and non-urban storm events

The MRG receives a variety of stormwater inputs from urban, non-urban, and mixed land-use watersheds. Some inputs are gauged, while others are not, making it difficult to clearly define the source of a given stormwater pulse from basic hydrometry values alone. We used the *EcoHydrology* R package (Fuka et al., 2018) to separate quickflow from baseflow using a threshold of 1.7 $m^3/s$ to extract hydrographs for analyses. This threshold was set based on visual analysis of discharge time-series for Alameda as high enough to remove diurnal variability, but low enough to capture small storm events. Once events were identified, we found two consistent and distinct patterns that allowed us to classify the origin of the storms, i.e.: 1) an urban storm event has direct runoff ≥1.7 $m^3/s$, and SpCond ≥50 μS/cm below pre-event baseline conductivity, and 2) a non-urban event is defined by direct runoff ≥1.7 $m^3/s$, and SpCond ≥50 μS/cm above pre-event baseline conductivity. We did not include any events where return to baseline SpCond was not clearly achieved. In total, 15 discrete storm events were identified and analyzed: 10 urban events and 5 non-urban events.

### 2.4. Modeling dissolved oxygen

We used two methods to estimate dissolved oxygen concentrations for two separate applications. In the first method, we estimated DO from temperature data to interpret whether changes in temperature during storm events could account for DO variations. For this, a linear regression equation was fitted to DO versus temperature data for multiple periods of baseflow. Next, this equation ($DO\ (mg/L) = -0.123 * Temp\ (C) + 9.937$) was used to predict and compare DO values during storm events.

Second, we used transfer-function modeling (Young, 2006) to predict conservative (i.e., non-reactive) DO transport from SpCond time-series (Fig. S2) along a 21 km reach between the Alameda (upstream) and Rio Bravo (downstream) sites. Because urban and non-urban storms originate in different places within the MRG, and there are a large number of ungauged potential inputs, we are unable to clearly define watershed boundaries or transit times for most events. This makes it difficult to directly compare urban and non-urban storm events that originate in different places and interpret potential differences or similarities in drivers of DO sags using traditional modeling approaches. To address this, we used transfer-function models, which are data-based and do not require information on storm pulse origin. In this way, we eliminate uncertainty regarding storm source from our modeling efforts. To construct the transfer function, we used data from the upstream site (Alameda, Fig. 1) for a quantity that acts conservatively from a biological perspective (i.e., SpCond), to model the downstream signal (Rio Bravo, Fig. 1). The models used to derive transfer functions are shown in Fig. S2. Next, we applied these established transfer functions to DO using the upstream DO signal from Alameda, to predict what the DO signal at the downstream Rio Bravo site would have been if the transport had been conservative. We then compared the actual measured DO time-series (non-conservative) to modeled DO time-series (conservative), to interpret net oxygen consumption (i.e., instances with lower observed DO than predicted by the conservative transfer-function model) and net oxygen production/reaeration (i.e., higher observed DO than by the conservative transfer-function model). This modeling approach was conducted using routines in the CAPTAIN Toolbox (Young et al., 2010) for Matlab (The MathWorks, Inc., Natick, MA) available at http://captaintoolbox.co.uk/. Additional details describing modeling workflow can be found in Supplemental Information.

### 2.5. Statistics

Data management and analysis, as well as plotting Figs. 2, 4 and 5 using the *ggplot2* package (Wickham, 2016), were conducted in R.

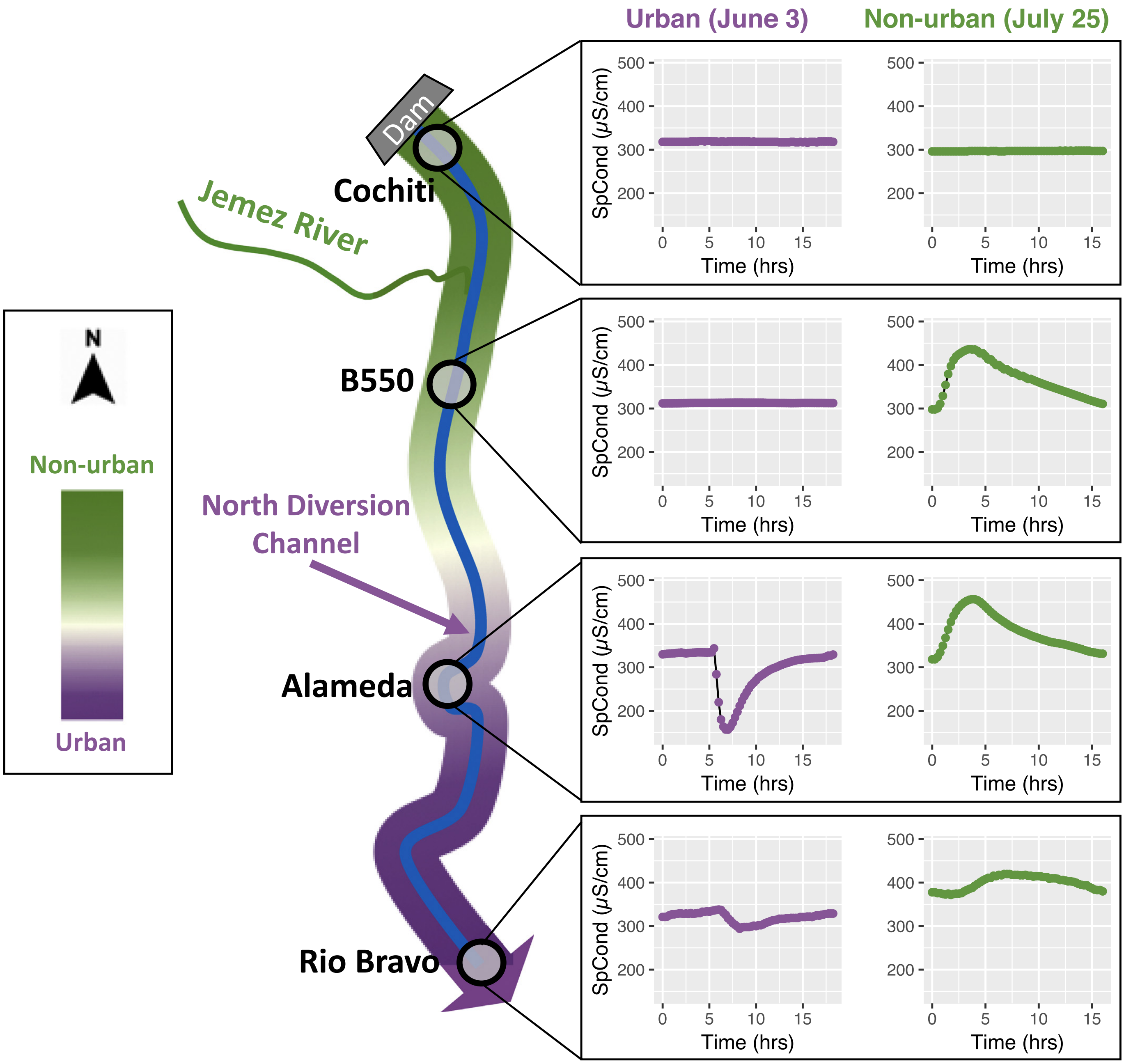


**Fig. 2.** Time-series for specific conductivity (SpCond) signatures for one urban storm (June 3, purple) and one non-urban storm (July 25, green) are shown for four stations located along the Middle Rio Grande flowpath. Storm signatures were lagged to account for travel time between sites so that all purple SpCond traces represent the same urban storm, and all green SpCond traces represent the same non-urban storm. The difference in SpCond patterns is used to identify urban and non-urban events. (For interpretation of the references to color in this figure legend, the reader is referred to the web version of this article.)

Statistical tests and plotting of additional figures were conducted in JMP®, Version 13 (SAS Institute, Cary, NC). For initial comparison of storms, we used delta (∂) values using the maximum and minimum values for each water quality parameter and event. For spikes, ∂ = maximum – minimum, and for sags, ∂ = minimum – maximum. In addition, we calculated area under the curve (AUC) statistics using the *caTools* package (Tuszynski, 2019). While the ∂ approach provides a quantitative metric of the extreme values of a given event, the AUC approach better incorporates the time-varying component of each storm. For all these storms, the direct runoff volume contribution was estimated using the area under the baseflow-removed discharge vs time hydrograph.

We used endmember mixing of the SpCond signal to determine the percentage of total river discharge contributed by urban runoff for each urban storm event. We used baseline SpCond values to establish the river endmember (Fig. S3), and the runoff endmember was approximated as conductivity of 20 μS/cm previously reported for rainfall (Sequeria and Lung, 1995). Because we interpret fDOM as a proxy for DOC and turbidity as a proxy for TSS throughout the manuscript, we collected grab samples for DOC and TSS during storm events to calibrate fDOM:DOC and turbidity:TSS proxy relationships and validate these assumptions. The correlation between fDOM (measured in situ) and DOC (measured in the laboratory) represents an fDOM range of 33–90 QSU, and is both strong and highly significant ($r = 0.95$, $p < 0.0001$, $n = 14$). The correlation between turbidity (measured in-situ) and TSS (measured in the laboratory) to calibrate the turbidity:TSS ratio represents a turbidity range of 147–10,663 FNU, and is both strong and highly significant ($r = 0.96$, $p < 0.0001$, $n = 29$). For principal component analysis

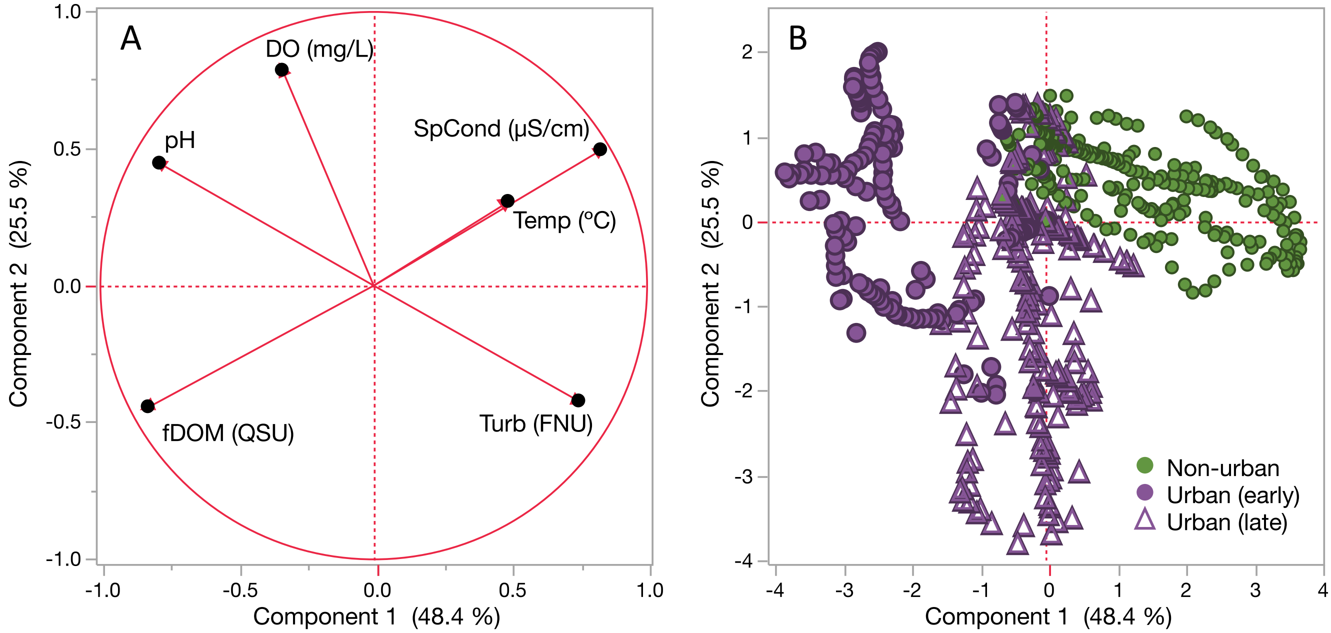


**Fig. 3.** Principal component analysis (PCA) of normalized water quality data for dissolved oxygen (DO), fluorescent dissolved organic matter (fDOM), pH, specific conductivity (SpCond), turbidity (Turb), and temperature (Temp) for urban and non-urban events in Table 1 (5/21, 6/3, 6/16, and 7/25 events removed due to missing data). The loading plot (A) presents the correlations between each water quality parameter and either principle component 1 (PC1) or principal component 2 (PC2), while the score plot (B) shows the division between urban and non-urban events on PC1, and the division of early-season (July 30th, August 1st and 2nd) and later-in-season urban events along PC2. Because scores are normalized, parameters are unitless, where original units are provided for reference.

(PCA), data for each storm were normalized between −1 and 1 for each parameter. Baseline values were set to 0, while maximum spike values were set to 1, and minimum sag values were set to −1. This was done for all parameters included in the PCA, to remove the effect on the analysis of large differences in range between individual storms. We note that fDOM data for non-urban events are excluded from Table 1 as it was deemed unreliable, and that storms missing data for one or more parameters as shown in Fig. S5 (i.e., the first three storm events) were excluded from the PCA. It is also important to note that we included non-urban fDOM in the PCA to allow for direct comparison between urban and non-urban water quality using the full suite of parameters. For correlation statistics throughout the manuscript, we use a significance threshold of $p < 0.05$, and report continuous $p$-values following guidance by Wasserstein et al. (2019). Correlation statistics are reported as correlation coefficients ($r$), and classified as weak ($0.3 \geq r \geq 0.5$), moderate ($0.5 \geq r \geq 0.7$), and strong ($r \geq 0.7$).

### 2.6. Literature review for results contextualization

We conducted a literature review focused on gathering information about water quality responses in urban runoff across a broad range of biomes. Studies were only included if they met three criteria: 1) storm events were specifically reported, not just baseflow, 2) the method in which the data were presented allowed for interpretation of clear temporal patterns depicting a given water quality parameter increasing, decreasing, or both, and 3) provided information for at least one of the water quality parameters of interest. Included studies span a broad range of rainfall regimes, which we used to ask the question: are water quality signatures in urbanized catchments consistent across biomes? We divided environments into wetter and drier using a threshold of 700 mm annual rainfall, where Albuquerque is the driest location reported, and compared average responses between wetter and drier regions, and for the table as a whole. Results from the current

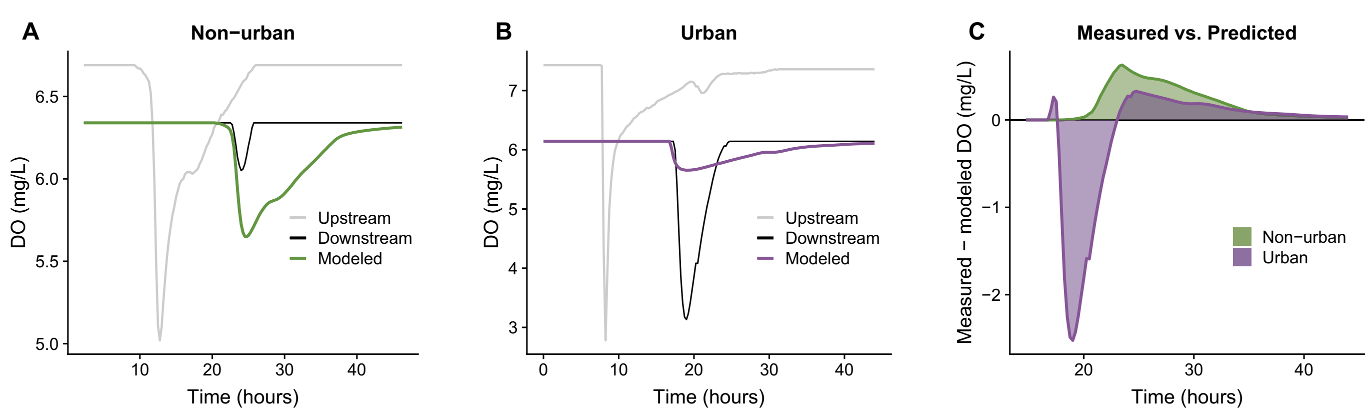


**Fig. 4.** The transfer functions calibrated from the signal variation of a conservative tracer (specific conductivity) between an upstream (Alameda) and downstream (Rio Bravo) site was used to model conservative transport of dissolved oxygen (DO) along the same reach after a non-urban (A) and an urban event (B). Comparing measured and modeled DO (C) demonstrates that the non-urban DO sag is smaller than predicted, while the urban DO sag is considerably larger than predicted.

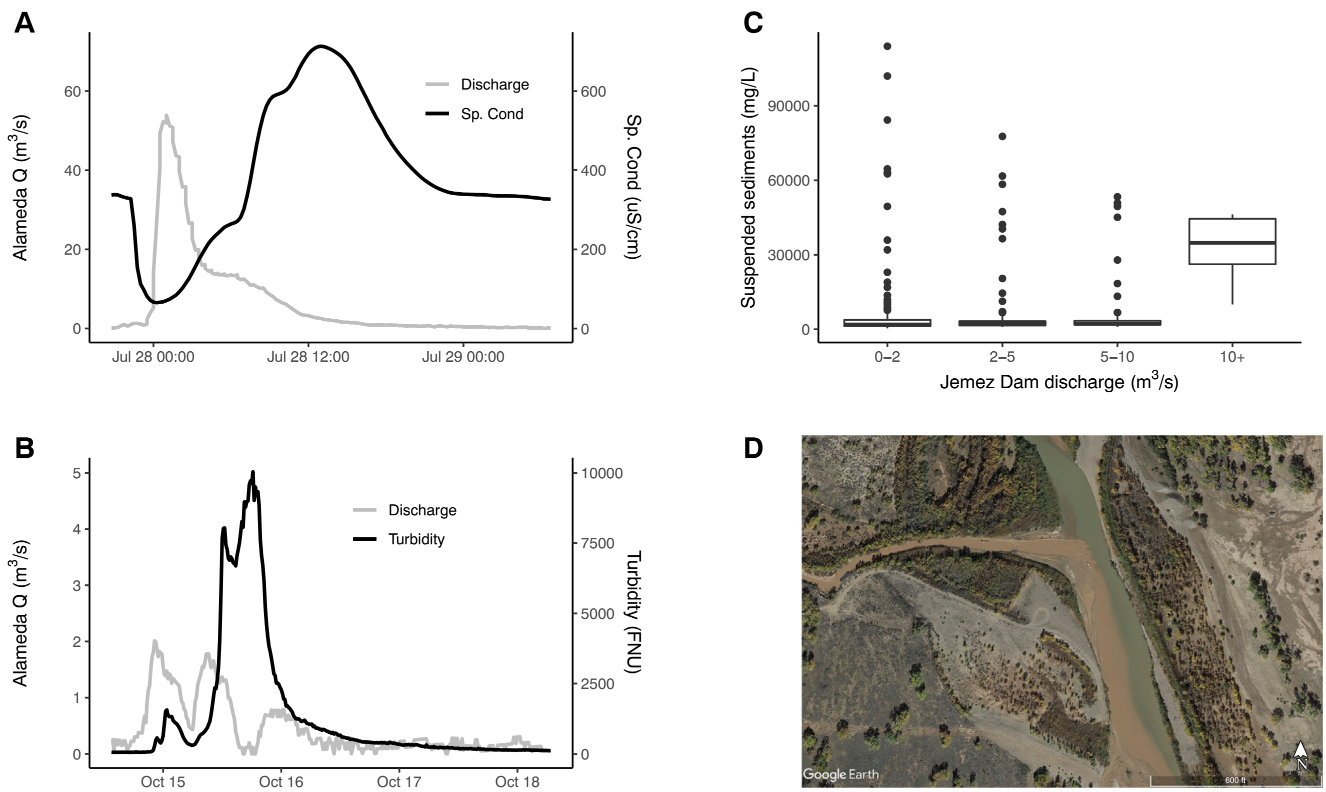


**Fig. 5.** Examples of dynamic responses of MRG water quality to complex hydrologic inputs during non-urban storm events. A) Overlapping urban and non-urban events measured at Alameda, distinguished by specific conductivity (SpCond) rather than by discharge provide a clear example of rapid changes in water quality based on runoff source. B) A large turbidity spike and minimal discharge increase measured at Alameda during a non-urban event. C) A comparison of discharge and suspended sediment concentrations (SSC) from the Jemez River, a tributary to the MRG demonstrating highest turbidity values during lowest flows, and D) an aerial photo (Google Earth v7.3.2.5776) of the confluence of the Jemez River and Rio Grande showing mixing of highly turbid non-urban stormwater inputs with sediment-depleted MRG waters below Cochiti.

study are based on average values for water quality responses at Alameda, as presented at the bottom of Table 1.

## 3. Results

### 3.1. Water quality signatures for urban and non-urban events

The water quality parameters measured in this study are influenced by physical, chemical, and biological factors. For simplicity, we have divided these parameters into two categories based on the observed drivers in our system (Table 1, Fig. S3): physical (temperature, SpCond, and turbidity) and biogeochemical (DO, pH, fDOM and $NO_3$).

#### 3.1.1. Physical stormwater signatures

Fig. 2 presents time-series data of SpCond at our four monitoring sites in response to storm events originating in urban and non-urban sub-watersheds. For the urban storm, sags in the SpCond signatures are observed at Alameda and Rio Bravo. This storm coincides with a

**Table 1**
Storm event hydrology and water quality measured at Alameda.

| Date (m/d/yy) | Type | Physical properties | | | | Biogeochemical properties | | |
|---|---|---|---|---|---|---|---|---|
| | | Direct runoff[a] | ∂-SpCond | ∂-Temp | ∂-Turbidity | ∂-DO | ∂-pH | ∂-fDOM[b] |
| 5/21/18 | Urban | 230.70 | −202.83 | −10.70 | 529.36 | 2.58 | 0.25 | – |
| 6/3/18 | Urban | 153.57 | −186.70 | 4.87 | 200.10 | −4.65 | – | 265.63 |
| 6/16/18 | Urban | 210.19 | −238.93 | 3.51 | 213.65 | −5.65 | – | 300.43 |
| 7/30/18 | Urban | 344.70 | −262.52 | −10.49 | 2115.26 | −2.42 | 0.92 | 161.79 |
| 8/1/18 | Urban | 182.14 | −207.80 | 3.02 | −4774.73 | −2.97 | 0.40 | 80.21 |
| 8/2/18 | Urban | 87.31 | −98.25 | 1.62 | −2065.46 | −4.46 | 0.41 | 61.28 |
| 8/17/18 | Urban | 33.40 | −52.80 | 1.56 | 40.81 | −1.29 | −0.21 | 109.00 |
| 8/22/18 | Urban | 218.48 | −181.00 | 1.70 | 10,516.27 | −1.94 | −0.33 | 139.24 |
| 9/19/18 | Urban | 76.31 | −125.63 | 7.09 | 105.91 | −1.91 | −0.48 | 149.40 |
| 10/30/18 | Urban | 49.20 | −106.20 | −0.88 | 64.10 | −1.14 | −0.27 | 70.54 |
| 7/25/18 | Non-urban | 209.41 | 139.90 | −4.12 | 7628.05 | −0.67 | – | – |
| 8/1/18 | Non-urban | 61.26 | 269.27 | 4.28 | 11,040.62 | −3.02 | −0.43 | – |
| 8/11/18 | Non-urban | 106.79 | 967.15 | 3.02 | 8099.33 | −1.80 | −0.16 | – |
| 8/18/18 | Non-urban | 68.62 | 695.50 | 4.69 | 7895.76 | −1.77 | −0.42 | – |
| 10/15/18 | Non-urban | 41.29 | 1218.65 | 1.58 | 8881.19 | −0.35 | −0.18 | – |
| | Average urban | 150.59 | −162.20 | 1.33 | 712.88 | −2.94 | 0.06 | 148.61 |
| | Average non-urban | 97.47 | 658.09 | 1.89 | 8708.99 | −1.52 | −0.30 | – |

[a] Reported as direct runoff excluding baseflow, in thousands of $m^3$.
[b] fDOM data were collected but not reported for non-urban events in Table 1 due to poor data quality.

strong discharge pulse from the North Diversion Channel, but may also represent additional inputs from other ungauged urban stormwater sources upstream of Alameda. All urban events show decreased conductivity (Table 1), with ∂ values ranging from −52.80 to −238.93 μS/cm. In contrast, the SpCond signatures for the non-urban storm in Fig. 2 exhibit consistent spikes for all sites except Cochiti, and coincide with a discharge event from the non-urban Jemez River watershed, but may also represent additional inputs from other ungauged non-urban stormwater sources upstream of Alameda. Consistent with Fig. 2, all non-urban events in Table 1 show increased conductivity. Non-urban event ∂ values range from +139.90 to +1218.65 μS/cm, with the largest ∂ value for non-urban SpCond being more than five times greater than the largest ∂ value for urban SpCond (Table 1).

Direct runoff volumes associated with urban and non-urban events are also presented in Table 1, where urban events range from 33,400 to 344,697 $m^3$ and non-urban events range from 61,255 to 209,414 $m^3$. On average, the direct runoff volume for urban storms is 150% greater than for non-urban storms. Two distinct relationships between SpCond and direct runoff volumes are present for urban and non-urban events. The non-urban storms exhibit a weak, non-significant negative correlation between ∂-SpCond and direct runoff volumes ($r = -0.38$, $p = 0.281$, $n = 5$). The urban storm events exhibit a strong, highly significant negative correlation between ∂-SpCond and direct runoff volumes ($r = -0.92$, $p = 0.0001$, $n = 10$). Based on endmember mixing using SpCond, maximum values for the percentage of total river discharge contributed by urban runoff ranged from 17% to 78%, with an average across all storms of 25%. We note that this statistic includes tails and pre-storm baseline values. Further, it is unlikely that the conductivity of water entering the Rio Grande after significant contact with impervious and semi-pervious surfaces during runoff is as low as pure rainwater, suggesting our calculations are under-estimates of the percentage of total river discharge contributed by urban stormwater inputs.

Temperature increased during the majority of storm events during peak stormflow (Table 1, Fig. S3), ranging from +1.56 to +4.87 °C. However, three urban events show decreased temperatures during storms, including two events with large (>10 °C) decreases. Four of five non-urban events show increased temperatures.

Turbidity generally increased during both urban and non-urban storm events (Table 1). However, the average increase in turbidity for non-urban storms was an order of magnitude larger than urban storms. All ∂-Turbidity values for urban events (with the exception of August 22) were smaller than any non-urban ∂-Turbidity. In addition, turbidity decreased during two urban events (August 1 and 2) associated with peak stormflow. We note that two consecutive storms (both labeled August 1 in Table 1) capture rapid changes in turbidity associated with a shift from an urban storm (decrease of 4775 FNU) to a non-urban storm pulse (increase of 11,041 FNU) within 24 h.

#### 3.1.2. Biogeochemical stormwater signatures

Dissolved oxygen (DO) concentrations show consistent decreases for all non-urban and urban events, except for one urban event on May 21 (Table 1), which also featured the largest temperature sag. On average, DO sags for urban storms were considerably larger than non-urban storms (~200%, Table 1), particularly earlier in the monsoon season. To test if DO sags can be explained by relatively consistent positive ∂-Temp storm responses, we fitted a correlation between DO and temperature during baseflow conditions. We then predicted DO values based on this regression model, and compared measured minimum DO and the predicted DO value for the same time-point. Results are presented in Fig. S4 and clearly demonstrate that all measured DO minima were lower than predicted by temperature alone, with an average difference of 2.65 mg/L for all events. For all non-urban and urban events, DO minima averaged 1.81 and 3.11 mg/L lower than predicted, respectively. Thus, temperature-dependent changes in oxygen solubility during storm events was unable to account for DO minima, particularly during urban events.

Consistent sags in pH were observed for all non-urban events, while both sags and spikes were observed for urban events (Table 1). Negative ∂-pH values are consistent with rainfall inputs, which has a lower pH (~5.5) than Rio Grande baseflow (~8.5). Positive ∂-pH values for urban storms all occur earlier in the season (May–early August), while all negative ∂-pH responses for urban events occur later in the season (mid-August–October).

Fluorescent dissolved organic matter (fDOM) decreased during all non-urban events, and increased during all urban events (Table 1, Fig. S3). The decrease in fDOM, an optical measurement, during all non-urban events is attributed to high levels of signal attenuation (light scattering from suspended particulates). Although these data are corrected for turbidity interference using an algorithm designed for highly turbid systems (potentially usable up to 6000 FNU), the extreme levels of turbidity during non-urban events (average increase of 8709 FNU) is beyond the scope of our correction, and we do not report fDOM for any non-urban events (Table 1), although we do include non-urban fDOM in the PCA. Turbidity corrections for fDOM for urban storms were satisfactory, as all urban events except for August 22 have turbidity values well below the 6000 FNU threshold. In connection with fDOM, both $NO_3$-N and $A_{254}$ were measured, although data were compromised by interference by turbidity for all storm events except the June 3 and June 16 urban storms. Data for $NO_3$-N and $A_{254}$ for these events are presented in Fig. S5, and show increases in both constituents, consistent with increases in fDOM (Table 1).

### 3.2. Principal component analysis

We used principal component analysis to examine the relationships between the water quality parameters presented in Table 1, and how they explain differences between urban and non-urban events (Fig. 3). The PCA explains 73.9% of variability within the dataset (Fig. 3A). PC1, which explains almost half the variability (48.4%), exhibits strong loadings (>|0.4|) for four of six variables (SpCond, pH, turbidity, fDOM), with the strongest positive loading for SpCond, and strongest negative loading for fDOM. PC2, which explains a quarter of the dataset variability (25.5%), only exhibits strong loadings (>|0.4|) for SpCond and DO (Fig. 3A). Based on the score plot (Fig. 3), urban and non-urban events almost completely separate along PC1, with an average PC1 value of −1.15 for urban events, and an average PC1 value of 1.91 for non-urban events. Similarly, non-urban events on average exhibit a more positive PC2 value than urban events (0.36 and − 0.81, respectively). The PCA also separates urban events into two categories, divided into early-season and later-in-season groups, where early-season urban storms (July 30, August 1 and August 2 events) exhibit more negative PC1 and more positive PC2 values, while later-in-season urban storms (August 17 & 22, September 19 and October 30 events) are characterized by more positive PC1 and more negative PC2 values (Fig. 3).

### 3.3. Transfer function modeling

As shown in Table 1, DO declined during peak runoff for all but one storm event and urban events consistently exhibit larger sags than non-urban events. Based on regression analysis, DO sags cannot be explained by concurrent increases in temperature (Fig. S4). Results in Fig. 4 clearly demonstrate different behavior between the urban and non-urban storms. For the non-urban storm, the modeled DO sag is considerably lower than the measured DO sag (Fig. 4A), and so DO concentrations are higher than predicted by conservative transport. In contrast, the modeled DO sag is much smaller than the measured DO sag for the urban storm event (Fig. 4B). This stark difference in oxygen demand is apparent in Fig. 4C, where the non-urban event is consistently positive (indicating more oxygen present than predicted by conservative

**Table 2**
Literature reports of water quality responses to urban stormwater runoff across a gradient of annual precipitation.

| Rainfall (mm/yr) | Type | Temperature | Sp. conductivity* | Dissolved oxygen | pH | Turbidity/TSS[a] | FDOM/DOC[b] | Nitrate | Reference |
|---|---|---|---|---|---|---|---|---|---|
| 3810 | Wetter | Decreased | Increased | Both | Decreased | Increased | Increased[b] | Increased | Jensen et al., 2014 |
| 1793 | Wetter | Increased | Both | – | – | – | – | – | Wengrove and Ballestero, 2012 |
| 1473 | Wetter | – | – | – | – | Increased | – | – | Mallin et al., 2009 |
| 1364 | Wetter | – | Decreased | Increased | Decreased | Increased | – | – | Butler and Vasconcelos, 2015 |
| 1263 | Wetter | – | – | – | – | Increased | – | – | Peters, 2009 |
| 1067 | Wetter | Increased | Decreased | Decreased | Both | Increased | – | – | Hasenmueller et al., 2017 |
| 1033 | Wetter | – | Decreased | – | – | – | – | – | Inserillo et al., 2017 |
| 838 | Wetter | – | Increased[§] | – | – | – | Increased[b] | Increased | Long et al., 2017 |
| 763 | Wetter | – | – | – | – | Increased[a] | – | – | Métadier and Bertrand-Krajewski, 2012 |
| 750 | Wetter | – | Decreased | – | – | – | – | Decreased | Schwientek et al., 2013 |
| 735 | Wetter | Increased | Decreased | Decreased | Decreased | Increased | Increased[b] | Decreased | Bhurtun et al., 2019 |
| 683 | Drier | – | Decreased | Decreased | – | Increased | – | – | McGrane et al., 2017 |
| 650 | Drier | – | Decreased | Decreased | Increased | Increased | Increased[b] | Decreased | Halliday et al., 2015 |
| 648 | Drier | – | Decreased | – | Decreased | Increased[a] | Increased[b] | – | Hatt et al., 2004 |
| 515 | Drier | Decreased | Decreased | Increased | Decreased | Increased[a] | – | Both | Barałkiewicz et al., 2014 |
| 475 | Drier | – | – | – | – | Increased | – | – | Melcher and Horsburgh, 2017 |
| 475 | Drier | – | – | – | – | – | Increased | – | Mihalevich et al., 2017 |
| 457 | Drier | – | Decreased | Decreased | – | Increased | – | – | Gray, 2004 |
| 412 | Drier | – | Increased | – | Decreased | Decreased | Increased[b] | Increased | Ortiz-Hernandez et al., 2016 |
| 310 | Drier | – | Decreased[§] | – | – | – | Decreased[b] | Increased | Gallo et al., 2013 |
| 217 | Drier | – | – | – | – | – | Increased[b] | – | Wise et al., 2019 |
| 217 | Drier | Increased | Decreased | Decreased | Increased | Increased | Increased | Increased | This study |

* Based on $Cl^-$ concentration.
[a] TSS.
[b] DOC/TOC.

transport), while DO values are lower than predicted during the urban storm peak, indicative of high oxygen demand.

### 3.4. Comparing urban stormwater signatures across biomes

The results presented above represent a considerable number of individual monsoon storm events from both urban and non-urban watersheds in a large arid-land river. Because studies of urban arid-land stormwater dynamics are more limited than equivalent studies in mesic systems, we conducted a literature review to provide a broader context for our findings. In Table 2, we present a number of studies reporting one or more of the water quality constituents we measured for an urban watershed. In general, the majority of reported studies found similar water quality responses in urban runoff, regardless of local climate.

## 4. Discussion

### 4.1. Differences in non-urban and urban water quality signatures

#### 4.1.1. Physical differences in water quality responses

Increased conductivity during non-urban storms is linked to high salt inputs from semi-pervious soils with low vegetation cover characteristic of desert watersheds, where, when evaporation rates exceed rainfall rates, salt accumulates within surficial soil layers (Gran et al., 2011). Low vegetation coverage is also linked to higher soil temperatures (Lozano-Parra et al., 2018), further increasing evaporation and subsequent concentration of salts. We link SpCond and temperature patterns during non-urban storms to these desert soil characteristics, where flushing of salt and heat transfer from soils drive increases in both parameters. Moreover, desert landscapes are predicted to have low infiltration capacity, as well as very low bank stability (Dodds et al., 2015), matching extreme turbidity values for non-urban events. High turbidity levels are sustained well downstream of non-urban inputs because sediments in the Rio Grande exhibit a high proportion of fine, easily suspended particles (~67% <0.0625 mm in diameter based on data from 1969 to 2019 from USGS gauge #08330000 on the Rio Grande at Albuquerque) relative to other major rivers (Saraceno et al., 2017). Such high turbidity levels are consistent with other semi-arid rivers including the Pecos River in New Mexico, USA (Huey and Meyer, 2010) and the Mara River in Kenya (Dutton et al., 2018).

In contrast to the non-urban storm pulses, the decreased conductivity associated with urban events is due to low conductivity rainfall combined with minimal soil inputs from largely impervious catchments, which reduce the ionic strength of runoff both here and in other urban systems (Barałkiewicz et al., 2014; Hasenmueller et al., 2017). Similarly, the average change in turbidity for urban events, which was almost an order of magnitude smaller than for non-urban events, is consistent with minimal soil inputs. The increased water temperature for seven of the urban storm pulses is not surprising as urban areas function as heat islands (e.g., Hendel et al., 2015), where impervious surfaces absorb and transfer more heat than natural surfaces (e.g., Thompson et al., 2008). Combined with other anthropogenic factors that increase thermal energy absorbance (Nelson and Palmer, 2007), higher average stream temperatures are generally observed for urban regions (Somers et al., 2013). These results match the urban stream syndrome framework, which predicts higher water temperatures in urban streams (Walsh et al., 2005). The decline in water temperature during some storm events is of interest and has been reported for urban stormwater runoff in other areas (Barałkiewicz et al., 2014, Bhurtun et al., 2019, Hatt et al., 2004; Inserillo et al., 2017, Jensen et al., 2014). One potential explanation for the two sizeable decreases in urban event temperature (May 21 and July 30) is increased evaporative cooling with wetting of hot impervious surfaces (Thompson et al., 2008); however, it is unclear why this mechanism would cause decreases in water temperature for some storms and not others.

#### 4.1.2. Biogeochemical differences in water quality responses

Sags in pH values for all non-urban events are consistent with the acidic pH of rainwater (~5.7) diluting river flows, where the pH of the Rio Grande is basic by comparison (average pH of 8.5 during baseflow at Alameda for the study period). Sags in DO are more complicated to explain. In pervious and semi-pervious catchments, groundwater can be a larger source of event-related flow than rainfall (Klaus and McDonnell, 2013 and references therein), with a report from one semi-arid catchment suggesting that groundwater comprised 64–98% of the total runoff following a precipitation event (Camacho Suarez et al., 2015). The interface between surface and groundwater in freshwater systems can drive strong biogeochemical gradients, and sharp decreases in both oxygen and pH have been associated with this boundary (e.g., Carling et al., 2019). Therefore, the consistent sags in pH and DO may be explained by a combination of direct runoff (that incorporates increased SpCond, turbidity, temperature and low pH) and groundwater (associated with very low DO and circumneutral pH). Another explanation for low DO is increased biological or chemical oxygen consumption in the water column or sediments (e.g., Dahm et al., 2015) driving higher oxygen demand. Increased oxygen demand is commonly observed during storm events (Lee and Bang, 2000), and is associated with increased nutrients or carbon (e.g., Mallin et al., 2009). This hypothesis is explored in great detail later in the manuscript, however, due to the lack of reliable fDOM and $NO_3$ data for non-urban storms, we are unable to directly compare nutrient and carbon dynamics between urban and non-urban storms. It is possible that upstream non-urban nutrient sources drive increased oxygen demand during storm events (albeit to a lower extent than urban events). For instance, non-urban watersheds draining into the MRG contain forested uplands and soil carbon-rich open bottomlands, both of which store more carbon and nitrogen compared to upland desert ecosystems (Dodds et al., 2015; McKenna and Sala, 2016; Peters and Gibbens, 2006). However, our quantitative comparison of oxygen demand using transfer function modeling, and the results discussed in detail below, provide limited evidence of oxygen demand in non-urban events.

In contrast to non-urban storms, we observed a change in pH patterns for urban storms where early-season storms showed pH spikes. Increased pH is not consistent with exchange of lower pH groundwater or acidic rainfall inputs. Instead, we suggest that alkaline inputs from impervious surfaces explain increased pH in urban stormflow. The NDC network and other stormwater conveyances draining into the Rio Grande are largely lined with concrete, and runoff contacting concrete has higher pH relative to other impervious surfaces (Pilon et al., 2019). As the monsoon season progresses, concrete surfaces are repeatedly flushed, and easily mobilized alkaline inputs from drainage channels decrease, resulting in more negative ∂-pH values throughout the monsoon season. Previous research also suggests that acidic rainfall can mobilize metals, including copper and zinc into urban runoff (Wicke et al., 2014). During early-season storms, increased pH levels may reduce the risk of leaching these metals (e.g., Salomons and Förstner, 1984), while this risk increases with lower pH values during late-season storms.

DO sags were, on average, considerably lower for urban storms than non-urban storms (Table 1), but are not easily explained by groundwater inputs as the urban watershed is largely impervious (Fig. 1). Instead, we suggest these sags are due to increased oxygen demand driven by considerable inputs of organic carbon and nutrients. Clear increases in fDOM act as a proxy for increased dissolved organic carbon (DOC) and are consistent with other studies characterizing urban runoff (Halliday et al., 2015; Hatt et al., 2004; Long et al., 2017; Bhurtun et al., 2019). Higher levels of DOC in urban runoff, including microbially produced DOC (Wise et al., 2019), are expected to increase biological oxygen demand (BOD) by heterotrophic microbial communities processing organic matter, where increased presence of labile DOC has been linked to increased efficiency of microbial process rates (Newcomer et al., 2012). A previous study of stormwater infrastructure's influence on runoff chemistry found imperviousness was linked to higher export of organic carbon and nitrogen (Hale et al., 2015).

### 4.2. Biological versus physical controls of water quality

Differences in soil characteristics explain distinct urban and non-urban water quality responses, where non-urban semi-pervious soils yield large inputs of salt, sediments and low-DO groundwater. In contrast, impervious surfaces limit sediment and salt inputs from the urban landscape while pH signatures indicate alkaline inputs from concrete conveyance channels. Consistently larger DO sags for urban events relative to non-urban events indicate increased oxygen demand associated with increased nutrient and organic matter. As such, explanations for the unique water quality signatures of urban and non-urban storm events primarily relate to biogeochemical versus physical drivers, respectively. PC1 in Fig. 3, which divides storms by type, also divides water quality parameters by physical versus biogeochemical. We note that the stormwater drainage conveyance networks in the study area are separated from the sewage network. This is an important distinction, because discharge from combined sewer overflows (CSOs) during storms is associated with increased nutrients and oxygen demand in receiving waters (Miskewitz and Uchrin, 2013). However, CSOs in the United States are clustered primarily in the northeast and northwest US, and are absent throughout arid regions of the southwest (Environmental Protection Agency, 2004). It is interesting, therefore, that patterns associated with the arid urban landscape independent of sewage inputs (i.e., increased nutrients, decreased oxygen) are similar to environmental impacts commonly associated with CSOs. Temperature, SpCond, and turbidity are all primarily controlled by physical processes (dilution, sediment dynamics, thermal properties) and all load positively on PC1 with non-urban events. Variables related to chemical and biological processes (DO, pH, fDOM) are all loaded negatively on PC1 with urban events. Division of storm event types by physical versus biogeochemical properties indicates the difference in drivers of urban and non-urban stormwater quality.

We quantified this distinction using transfer function modeling to directly compare urban and non-urban DO behavior, because we hypothesized that DO sags were likely due to biological or chemical factors, including nutrient enrichment and increased microbial activity. High oxygen demand for the urban event is consistent with increased nutrients and carbon (i.e., $NO_3$ and fDOM) present in urban runoff (Fig. 4). This suggests continued oxygen demand during transit, in spite of the high likelihood that reaeration during transport (equivalent to that observed for the non-urban event) reincorporates oxygen into the water column. Conversely, no clear oxygen demand and apparent reaeration in the non-urban event are consistent with physical factors controlling non-urban runoff. DO concentrations are strongly tied to reaeration, where exchange between the water column and the atmosphere maintain equilibrium, which explains apparent source behavior. Because we compared DO transport along the same stretch of river for both events in Fig. 4, the difference in oxygen demand is linked to either chemical or biological differences in runoff, and may indicate mobilization of highly active microbes from the urban landscape or stimulation of autochthonous microbial communities. Unpublished DOC lability data collected during a 28-day incubation found that only ~17% of DOC in surface waters at Alameda were consumed by local microbial communities, even when supplemented with $NO_3$ and $PO_4$ to remove any nutrient limitation. Therefore, our data suggests that high oxygen demand in urban pulses associated with heterotrophic processing of organic matter and nutrients is driven primarily by allochthonous microbial communities flushed from the urban landscape and stormwater conveyance networks. Although we do not have direct measurements of microbial activity, previous reports on biological characteristics of stormwater from the North Diversion Channel suggest that runoff contains high levels of bacteria, labile organic matter, nutrients (nitrogen and phosphorus), and experiences 5-day oxygen demand up to 80 mg/L (Storms et al., 2015; Fluke et al., 2019; Wise et al., 2019). All of these factors support our theory that increased heterotrophic activity can explain the oxygen sags in urban runoff. Further, we examined our data for a correlation between DO and fDOM to substantiate this theory, and found a weak but highly significant negative correlation between the parameters for all urban storms ($r = -0.49$, $p < 0.0001$, $n = 918$). An alternative explanation for DO sags is that increased turbidity absorbs sunlight, raising temperatures which drive decreased DO levels. We first examined the relationship between DO and turbidity for all urban and non-urban storms, and found a very weak but significant negative correlation ($r = -0.24$, $p < 0.0001$, $n = 1390$). However, the slope of this relationship indicated that a decrease of 1 mg/L DO equated an increase in turbidity of 8547 FNU. Based on the average decrease in DO and increase in turbidity in Table 1, this relationship cannot explain the magnitude of urban DO sags (the average decrease of −2.94 mg/L DO would require an increase in turbidity of ~25,000 FNU, or approximately 35 times the average urban increase in turbidity presented in Table 1). However, the non-urban average DO sag magnitude of −1.52 mg/L would require an increase in turbidity of ~13,000 FNU, which is only 150% the average non-urban increase in turbidity of 8709 FNU (Table 1). Therefore, we suggest that a turbidity-driven increase in heat absorption may be partially responsible for DO sags associated with non-urban events.

### 4.3. Relevance of findings to other environments

#### 4.3.1. Complex non-urban water quality responses in the Rio Grande

One of the goals of this study was to better understand how urban and non-urban runoff quality in an arid-land river compared to other environments. Although distinct storm events presented in Table 1 have relatively consistent water quality signatures within storm type, several examples of urban and non-urban pulses overlapping were captured, though not reported as we were unable to satisfactorily separate into discrete events. Fig. 5A provides an example of this, where an urban event associated with a SpCond sag and clear discharge pulse precedes a large spike in SpCond consistent with a non-urban storm pulse. The shift from minimum SpCond (peak of urban inputs) to maximum SpCond (peak of non-urban inputs) occurs in <12 h. From the chemical responses that we have identified in this study, these co-eluting events represent a shift in water quality from primarily urban (high DOC and oxygen demand), to primarily non-urban (high sediment levels but low oxygen demand), a transition that occurs within hours. While other rivers see rapid changes in water quality, we believe the extreme responses observed in the MRG are relatively unique to arid-land rivers due to 1) very low summer flows in the river providing minimal dilution of storm events, 2) isolated, intense monsoon storms that produce localized runoff, and 3) flashy hydrographs related to relatively impervious surfaces in both urban and non-urban catchments.

Another relatively unique signature in our dataset is the presence of distinct non-urban water quality signatures where minimal change in discharge is present. Fig. 5B presents an example where stormflow peaks consecutively around the same magnitude (~2 $m^3/s$), and turbidity values vary disproportionally, increasing to ~2000 FNU after the first increase in flow but reaching 10,000 FNU after the second increase in flow. Fig. 5B suggests that large quantities of sediments can be mobilized during very small runoff events. To test this, we plotted 5 years of data for suspended sediment concentrations (SSC) for the Jemez River measured ~4 km upstream of the confluence with the Rio Grande at USGS gauge #08329000 (data from J. Brown, USGS). We divided SSC data into boxplots based on discharge measured ~1 km downstream of the SSC gauge at USGS gauge #08328950, presented in Fig. 5C. Although higher turbidity values are, on average, associated with highest flows, we note that the highest SSC values recorded for the full dataset fall in the lowest discharge group. Thus, even small precipitation events are capable of mobilizing large quantities of sediments from non-urban arid watersheds. To visualize the impact of non-urban runoff on downstream water quality, Fig. 5D presents an aerial photo of the confluence of the Jemez River and the Rio Grande, where the highly turbid plume is easily distinguished from the considerably less turbid waters of the MRG due to the high sediment trapping efficiency of Cochiti Dam (Davis et al., 2014). Although increased turbidity with increased flow is common across biomes, a comparison of in situ turbidity levels across a range of arid, semi-arid and non-arid rivers found all locations with turbidity values >2000 FNU were arid or semi-arid rivers, including the Rio Grande (Khandewal et al., 2020).

#### 4.3.2. Urban stormwater signatures are similar across biomes

The studies presented in Table 2 agree with general findings from the current study. More studies found increased temperature, decreased SpCond, decreased DO, increased turbidity/TSS, increased fDOM/DOC and increased nitrate. One difference is pH, where the majority of previous studies found a decrease in pH (Table 2). While our dataset was split between increased and decreased (Table 1), a large increase during the July 30 storm sways the average ∂-pH value to positive for all urban events. When we break down Table 2 into wetter and drier categories, sample sizes get considerably smaller, resulting in less clarity in the data. For instance, three studies in wetter regions show increased temperature, but only two drier studies report temperature changes, with one showing a decrease and the current study showing an increase. However, SpCond, DO and pH both consistently decrease for wetter and drier studies, and turbidity/TSS, fDOM/DOC and nitrate consistently increase. Thus, with the exception of pH, results in Table 2 generally suggest that 1) water quality responses between wetter and drier responses are similar, and 2) on average, the studies included in Table 2 collectively agree with findings in the current study.

In urban watersheds, a unique cocktail of anthropogenic chemicals (including nutrients, metals and pollutants) are flushed from highly impervious surfaces into artificially designed networks of drainage channels (Chadwick et al., 2006; Kaushal et al., 2018; Lintern et al., 2018). Because such alterations to the physical, chemical, and biological properties of watersheds that control runoff quality influence urban catchments, it is not surprising that our findings indicate 1) stark differences between urban and non-urban runoff, and 2) generally consistent urban patterns across a gradient of annual precipitation. Interestingly, finding consistent responses in urban stormwater chemistry (Table 2) suggests the potential to develop solutions to water quality problems in one urban system that apply to other urban systems, regardless of local precipitation patterns. As previously noted by Booth et al. (2016), we recognize that many inter-connected factors influence runoff characteristics for a given urban catchment, and while general commonalities across precipitation regimes in urban runoff quality suggest the ability to apply a management or engineering single solution to multiple urban watersheds, it is important to not over-simplify complex hydrobiogeochemical dynamics and recognize that any solution implemented should be tailored to site-specific characteristics, and carefully monitored for success.

### 4.4. Ecological and management implications

#### 4.4.1. Ecological implications

In Fig. 6 we summarize the differences in water quality impacts between urban and non-urban stormwater runoff and their implications for the Rio Grande. Generally, urban storms drive short-term degradation of water quality, increasing DOC and nutrient concentrations, and decreasing DO concentrations (Tables 1 and 2, Fig. S5). DO concentrations below 5 mg/L exceed the US EPA advisory level for protecting diversity of aquatic life in freshwater ecosystems (Chapman, 1986), and we found DO values in the river as low as 1.72 mg/L during one urban event (Fig. S3). Previous studies indicate that even short periods (<24 h) of low oxygen conditions can be harmful to aquatic life (Magaud et al., 1997; Mallin et al., 2009). In the MRG, this is of particular concern for the Rio Grande silvery minnow, an endangered species endemic to the MRG that is sensitive to low DO levels (USFWS, 2011). Moreover, urban runoff from Albuquerque contains additional potential pollutants, including metals, volatile and semi-volatile organic compounds, polyaromatic hydrocarbons, polychlorinated biphenyls, and pesticides (Shephard et al., 2019; Storms et al., 2015), all of which may also impact downstream ecosystems. In contrast to urban events, non-urban events do not appear to pose a significant ecological threat to the MRG based on biogeochemical data collected for this study, as observed nutrient concentrations are not elevated, and DO concentrations generally stay above the 5 mg/L threshold. We note again that data

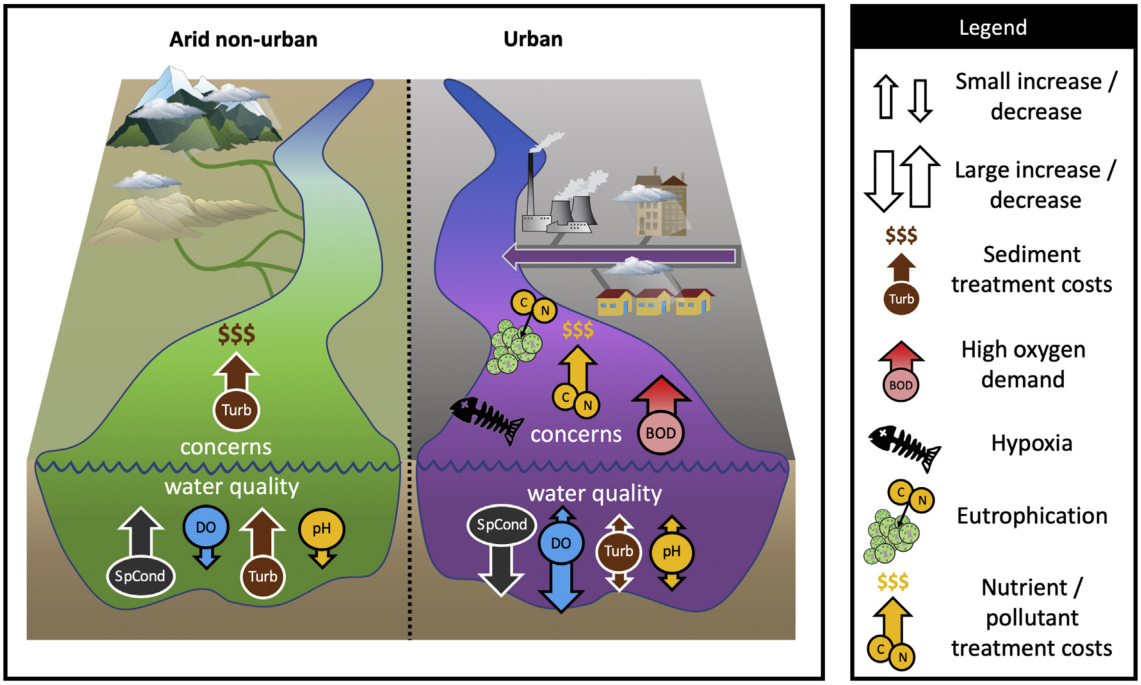


**Fig. 6.** Conceptual diagram summarizing changes for water quality parameters for non-urban events in the Rio Grande and urban events across biomes, summarized from Table 2. Potential concerns associated with changes in water quality are also presented.

quality for both nitrate and fDOM was consistently compromised during non-urban events, and therefore the ecological impacts of these constituents will not be interpreted.

Although high turbidity is a natural phenomenon in desert rivers, mobilization of sediments during non-urban storm events may have significant ecological impacts on the MRG. For instance, in sand-bed rivers like lower portions of the MRG, instability can lead to increased abrasion and scouring, particularly during high flows, that result in a reduction in primary productivity (Atkinson et al., 2008). High turbidity values limit light penetration in the water column, further limiting primary productivity (Davies-Colley and Smith, 2001, Summers, 2019), and can impact fish growth and potentially increase mortality (Bilotta and Brazier, 2008 and references therein). Moreover, settling of mobilized fine sediments can clog river beds, altering nutrient cycling and hyporheic exchange, and reducing habitat heterogeneity (Rehg et al., 2005, Drummond et al., 2017, 2018). In addition, suspended sediments are associated with various potential pollutants. For instance, in the nearby Pecos River watershed, Huey and Meyer (2010) found significant correlations between turbidity and E. coli in both non-urban and urban catchments, and recent research found that riverbed sediments control the sourcing of E. coli in the Rio Grande throughout seasons (Fluke et al., 2019).

*4.4.2. Management implications*

Arid-land rivers provide surface water to water-limited regions, and managing water quality is essential for drinking water security. In the MRG, as in many other arid-land rivers, very high levels of suspended solids increase treatment costs associated with lowering turbidity to drinking water standards. For example, Dearmont et al. (1998) estimated an average treatment cost of \$3.83 per million gallons per NTU reduced. This is significant since the Albuquerque Water Utility Authority diverts, on average, 35.46 million gallons per day (or ~370,000 gal every 15 min) from the Rio Grande (data from abcwua.org for 1/1/2015–9/24/2019). Even if intakes are generally shut down during storm events, there is potential that non-urban events, which are associated with minimal change in discharge but large changes in turbidity, may be difficult to detect, and some stormwater may enter the treatment process. We used the July 25th non-urban storm event, with mean turbidity of 3045 FNU (or 3045 NTU), to calculate the potential treatment costs for intake of turbid stormwater. Over the course of just 15 min, the intake of 370,000 gal of river water with average storm turbidity would cause an estimated treatment cost of \$4315. At peak storm turbidity for this same event (8214 FNU), that cost would more than double to \$11,639. If the storm pulse is not detected quickly, each additional hour that stormwater is pulled into the treatment system at peak turbidity could add as much as \$46,095 in additional treatment costs. Further, increased sediments are associated with other deleterious effects, including algae and other microorganisms (Matson et al., 1978), and related illnesses (Schwartz et al., 2000; Hsieh et al., 2015). The high fDOM values observed during urban events are also of concern for drinking water security, since high concentrations of organic matter have been linked to formation of disinfection byproducts (Rook, 1977; Chow et al., 2007; Beggs et al., 2009).

## 5. Conclusions

Urban and non-urban storms in the Rio Grande exhibited different water quality signatures associated with different drivers. We linked low DO (including short-lived hypoxia) during urban events primarily to oxygen demand, and suggest that increased inputs of fDOM and $NO_3$ present in urban runoff fueling heterotrophic activity are at least partially responsible. In contrast, non-urban storms are largely driven by physical processes, and do not show clear evidence of oxygen demand. However, the large suspended sediment loads associated with non-urban events pose a significant challenge to water supply managers.

Our results suggest that SpCond serves as an effective indicator of urban or non-urban stormwater in the MRG. Aside from early detection of urban on non-urban inputs based on the shape of the SpCond response (sag or spike), moderate fits between turbidity and SpCond for non-urban events ($R = 0.66$, $p < 0.0001$) and fDOM and SpCond for urban events ($R = -0.53$, $p < 0.0001$) suggest SpCond as an useful proxy for parameters that are more complex or more expensive to measure (i.e., optical measurements like turbidity, DOC and $NO_3$) as well as other contaminants associated with urban discharge, including disinfection byproducts linked to DOC, and other anthropogenic pollutants. The ability to use high-frequency in situ data collection to inform water resources management in real-time is increasingly recognized (e.g., Kerkez et al., 2016; Pellerin et al., 2016), and our findings indicate that, once properly calibrated, simple high-frequency measurements can serve as valuable proxies to guide adaptive (and potentially automated) decision making towards more effective water management, particularly in complex mixed land-use watersheds.

Findings from this study advance our knowledge of the relationships between land use and water quality in the Rio Grande. Due to the similarity of water quality responses across biomes to the patterns presented in this study, we suggest that our findings are broadly applicable across a range of environments, including mesic urban areas. However, we also report distinctive non-urban water quality phenomena and suggest these are unique to arid and semi-arid climates.

## CRediT authorship contribution statement

**Peter J. Regier:** Conceptualization, Software, Formal analysis, Writing - original draft, Funding acquisition. **Ricardo González-Pinzón:** Conceptualization, Formal analysis, Writing - review & editing, Supervision, Funding acquisition. **David J. Van Horn:** Conceptualization, Formal analysis, Writing - review & editing, Supervision, Funding acquisition. **Justin K. Reale:** Software, Writing - review & editing. **Justin Nichols:** Data curation, Writing - review & editing. **Aashish Khandewal:** Data curation, Writing - review & editing.

## Declaration of competing interest

The authors do not declare any conflict of interest in submitting this manuscript for publication.

## Acknowledgements

The National Science Foundation (grants CBET-1707042, HRD-1345169), including a postdoctoral fellowship to PR (HRD-1720912) and the US Army Corps of Engineers' Upper Rio Grande Water Operations Model (URGWOM, internal funding and cooperative agreement W912HZ-14-2-0014) provided support for this research. Any use of trade, firm, or product names is for descriptive purposes only and does not imply endorsement by the US Government. The findings and conclusions in this article are those of the authors and do not necessarily represent the views of the US Government.

## Appendix A. Supplementary data

Supplementary data to this article can be found online at https://doi.org/10.1016/j.scitotenv.2020.138443.

## References

Adams, D.K., Comrie, A.C., 1997. The North American monsoon. Bull. Am. Meteorol. Soc. 78 (10), 2197–2214. https://doi.org/10.1175/1520-0477(1997)078<2197:TNAM>2.0.CO;2.

Almakki, A., Jumas-Bilak, E., Marchandin, H., Licznar-Fajardo, P., 2019. Antibiotic resistance in urban runoff. Sci. Total Environ. 667, 64–76. https://doi.org/10.1016/j.scitotenv.2019.02.183.

Archdeacon, T.P., 2016. Reduction in spring flow threatens Rio Grande silvery minnow: trends in abundance during river intermittency. Trans. Am. Fish. Soc. 145 (4), 754–765. https://doi.org/10.1080/00028487.2016.1159611.

Atkinson, B.L., Grace, M.R., Hart, B.T., Vanderkruk, K.E.N., 2008. Sediment instability affects the rate and location of primary production and respiration in a sand-bed stream. J. N. Am. Benthol. Soc. 27 (3), 581–592. https://doi.org/10.1899/07-143.1.

Barałkiewicz, D., Chudzińska, M., Szpakowska, B., Świerk, D., Gołdyn, R., Dondajewska, R., 2014. Storm water contamination and its effect on the quality of urban surface waters. Environ. Monit. Assess. 186 (10), 6789–6803. https://doi.org/10.1007/s10661-014-3889-0.

Beggs, K.M.H., Summers, R.S., McKnight, D.M., 2009. Characterizing chlorine oxidation of dissolved organic matter and disinfection by-product formation with fluorescence spectroscopy and parallel factor analysis. J. Geophys. Res. Biogeosci. (G4), 114 https://doi.org/10.1029/2009JG001009.

Bhurtun, P., Lesven, L., Ruckebusch, C., Halkett, C., Cornard, J.-P., Billon, G., 2019. Understanding the impact of the changes in weather conditions on surface water quality. Sci. Total Environ. 652, 289–299. https://doi.org/10.1016/j.scitotenv.2018.10.246.

Bilotta, G.S., Brazier, R.E., 2008. Understanding the influence of suspended solids on water quality and aquatic biota. Water Res. 42 (12), 2849–2861. https://doi.org/10.1016/j.watres.2008.03.018.

Blythe, T.L., Schmidt, J.C., 2018. Estimating the natural flow regime of rivers with longstanding development: the northern branch of the Rio Grande. Water Resour. Res. 54 (2), 1212–1236. https://doi.org/10.1002/2017WR021919.

Booth, D.B., Roy, A.H., Smith, B., Capps, K.A., 2016. Global perspectives on the urban stream syndrome. Freshw. Sci. 35 (1), 412–420. https://doi.org/10.1086/684940.

Brix, K.V., Keithly, J., Santore, R.C., DeForest, D.K., Tobiason, S., 2010. Ecological risk assessment of zinc from stormwater runoff to an aquatic ecosystem. Sci. Total Environ. 408 (8), 1824–1832. https://doi.org/10.1016/j.scitotenv.2009.12.004.

Brooks, P.D, Haas, P.A., Huth, A.K., 2007. Seasonal variability in the concentration and flux of organic matter and inorganic nitrogen in a semiarid catchment, San Pedro River, Arizona. J. Geophys. Res. Biogeosci. (G3) 112. https://doi.org/10.1029/2006JG000275.

Butler, C.G., Vasconcelos, J.G., 2015. The effect of highway stormwater runoff on water quality in the little Cahaba Creek. World Environmental and Water Resources Congress 2015, pp. 2658–2666. https://doi.org/10.1061/9780784479162.261.

Camacho Suarez, V.V., Saraiva Okello, A.M.L., Wenninger, J.W., Uhlenbrook, S., 2015. Understanding runoff processes in a semi-arid environment through isotope and hydrochemical hydrograph separations. Hydrol. Earth Syst. Sci. 19 (10), 4183–4199. https://doi.org/10.5194/hess-19-4183-2015.

Carling, G.T., Romanowicz, E.A., Jin, L., Fernandez, D.P., Tingey, D.G., Goodsell, T.H., 2019. Redox conditions and pH control trace element concentrations in a meandering stream and shallow groundwater of a semiarid mountain watershed, Red Canyon, Wyoming, USA. Environ. Earth Sci. 78 (16), 510. https://doi.org/10.1007/s12665-019-8528-1.

Chadwick, M.A., Dobberfuhl, D.R., Benke, A.C., Huryn, A.D., Suberkropp, K., Thiele, J.E., 2006. Urbanization affects stream ecosystem function by altering hydrology, chemistry, and biotic richness. Ecol. Appl. 16 (5), 1796–1807. https://doi.org/10.1890/1051-0761(2006)016[1796:uasefb]2.0.co;2.

Chapman, G., 1986. Ambient Water Quality Criteria for Dissolved Oxygen (No. EPA 440/5-86-003).

Chavarria, S.B., Gutzler, D.S., 2018. Observed changes in climate and streamflow in the upper Rio Grande Basin. J. Am. Water Resour. Assoc. 54 (3), 644–659. https://doi.org/10.1111/1752-1688.12640.

Chow, A.T., Dahlgren, R.A., Harrison, J.A., 2007. Watershed sources of disinfection byproduct precursors in the Sacramento and San Joaquin Rivers, California. Environ. Sci. Technol. 41 (22), 7645–7652. https://doi.org/10.1021/es070621t.

Dahm, C.N., Candelaria-Ley, R.I., Reale, C.S., Reale, J.K., Horn, D.J.V., 2015. Extreme water quality degradation following a catastrophic forest fire. Freshw. Biol. 60 (12), 2584–2599. https://doi.org/10.1111/fwb.12548.

Davies-Colley, R.J., Smith, D.G., 2001. Turbidity suspended sediment, and water clarity: a review. J. Am. Water Resour. As. 37 (5), 1085–1101. https://doi.org/10.1111/j.1752-1688.2001.tb03624.x.

Davis, C.M., Bahner, C., Eidson, D., Gibson, S., 2014. Understanding reservoir sedimentation along the Rio Grande: a case study from Cochiti Dam. World Environmental and Water Resources Congress 2014, pp. 2347–2357.

Dearmont, D., McCarl, B.A., Tolman, D.A., 1998. Costs of water treatment due to diminished water quality: a case study in Texas. Water Resour. Res. 34 (4), 849–853. https://doi.org/10.1029/98WR00213.

Dettinger, M., Udall, B., Georgakakos, A., 2016. Western water and climate change. Ecol. Appl., 2069–2093 https://doi.org/10.1890/15-0938.1.

Ding, J., Jiang, Y., Fu, L., Liu, Q., Peng, Q., Kang, M., 2015. Impacts of land use on surface water quality in a subtropical river basin: a case study of the Dongjiang River Basin, Southeastern China. Water 7 (8), 4427–4445. https://doi.org/10.3390/w7084427.

Dodds, W.K., Gido, K., Whiles, M.R., Daniels, M.D., Grudzinski, B.P., 2015. The stream biome gradient concept: factors controlling lotic systems across broad biogeographic scales. Freshw. Sci. 34 (1), 1–19. https://doi.org/10.1086/679756.

Downing, B.D., Pellerin, B.A., Bergamaschi, B.A., Saraceno, J.F., Kraus, T.E.C., 2012. Seeing the light: the effects of particles, dissolved materials, and temperature on in situ measurements of DOM fluorescence in rivers and streams. Limnol. Oceanogr. Methods 10 (10), 767–775. https://doi.org/10.4319/lom.2012.10.767.

Drummond, J., Larsen, L., González-Pinzón, R., Packman, A., Harvey, J., 2017. Fine particle retention within stream storage areas at base flow and in response to a storm event. Water Resour. Res. https://doi.org/10.1002/2016WR020202.

Drummond, J., Larsen, L., González-Pinzón, R., Packman, A., Harvey, J., 2018. Less fine particle retention in a restored versus unrestored urban stream: balance between hyporheic exchange, resuspension, and immobilization. J. Geophys. Res. Biogeosci. https://doi.org/10.1029/2017JG004212.

Dutton, C.L., Subalusky, A.L., Anisfeld, S.C., Njoroge, L., Rosi, E.J., Post, D.M., 2018. The influence of a semi-arid sub-catchment on suspended sediments in the Mara River, Kenya. PLoS One 13 (2), e0192828. https://doi.org/10.1371/journal.pone.0192828.

Environmental Protection Agency, 2004. Report to Congress: Impacts and Control of CSOs and SSOs, Report No. 833-R-04-001. at. https://www.epa.gov/sites/production/files/2015-10/documents/csossortc2004_full.pdf, Accessed date: 30 March 2020.

Feng, S., Fu, Q., 2013. Expansion of global drylands under a warming climate. Atmos. Chem. Phys. 13 (19), 10081–10094. https://doi.org/10.5194/acp-13-10081-2013.

Fenn, M.E., Poth, M.A., Aber, J.D., Baron, J.S., Bormann, B.T., Johnson, D.W., ... Stottlemyer, R., 1998. Nitrogen Excess in North American Ecosystems: Predisposing Factors, Ecosystem Responses, and Management Strategies. Ecological Applications 8 (3), 706–733. https://doi.org/10.1890/1051-0761(1998)008[0706:NEINAE]2.0.CO;2 1998.

Fluke, J., González-Pinzón, R., Thomson, B., 2019. Riverbed sediments control the spatio-temporal variability of E. coli in a highly managed, arid river. Front. Water https://doi.org/10.3389/frwa.2019.00004.
Freeman, P.L., Schorr, M.S., 2004. Influence of watershed urbanization on fine sediment and macroinvertebrate assemblage characteristics in tennessee ridge and valley streams. J. Freshw. Ecol. 19 (3), 353–362. https://doi.org/10.1080/02705060.2004.9664908.
Fuka, D.R., Walter, M.T., Archibald, J.A., Steenhuis, T.S., Easton, Z.M., 2018. EcoHydRology: A Community Modeling Foundation for Eco-Hydrology (Version 0.4.12.1).
Galfi, H., Österlund, H., Marsalek, J., Viklander, M., 2017. Mineral and anthropogenic indicator inorganics in urban stormwater and snowmelt runoff: sources and mobility patterns. Water Air Soil Pollut. 228 (7), 263. https://doi.org/10.1007/s11270-017-3438-x.
Gallo, E.L., Brooks, P.D., Lohse, K.A., McLain, J.E.T., 2013. Land cover controls on summer discharge and runoff solution chemistry of semi-arid urban catchments. J. Hydrol. 485, 37–53. https://doi.org/10.1016/j.jhydrol.2012.11.054.
Gautam, M.R., Acharya, K., Stone, M., 2010. Best management practices for stormwater management in the desert southwest. J. Contemp. Water Res. Educ. 146 (1), 39–49. https://doi.org/10.1111/j.1936-704X.2010.00390.x.
Gran, M., Carrera, J., Massana, J., Saaltink, M.W., Olivella, S., Ayora, C., Lloret, A., 2011. Dynamics of water vapor flux and water separation processes during evaporation from a salty dry soil. J. Hydrol. 396 (3), 215–220. https://doi.org/10.1016/j.jhydrol.2010.11.011.
Gray, L., 2004. Changes in water quality and macroinvertebrate communities resulting from urban stormflows in the Provo River, Utah, U.S.A. Hydrobiologia 518 (1), 33–46. https://doi.org/10.1023/B:HYDR.0000025055.15164.40.
Hale, R.L., Turnbull, L., Earl, S.R., Childers, D.L., Grimm, N.B., 2015. Stormwater infrastructure controls runoff and dissolved material export from arid urban watersheds. Ecosystems 18 (1), 62–75. https://doi.org/10.1007/s10021-014-9812-2.
Halliday, S.J., Skeffington, R.A., Wade, A.J., Bowes, M.J., Gozzard, E., Newman, J.R., Jarvie, H.P., 2015. High-frequency water quality monitoring in an urban catchment: hydrochemical dynamics, primary production and implications for the Water Framework Directive. Hydrol. Process. 29 (15), 3388–3407. https://doi.org/10.1002/hyp.10453.
Hasenmueller, E.A., Criss, R.E., Winston, W.E., Shaughnessy, A.R., 2017. Stream hydrology and geochemistry along a rural to urban land use gradient. Appl. Geochem. 83, 136–149. https://doi.org/10.1016/j.apgeochem.2016.12.010.
Hatt, B.E., Fletcher, T.D., Walsh, C.J., Taylor, S.L., 2004. The influence of urban density and drainage infrastructure on the concentrations and loads of pollutants in small streams. Environ. Manag. 34 (1), 112–124. https://doi.org/10.1007/s00267-004-0221-8.
Hendel, M.A., Colombert, M., Diab, Y., Royon, L., 2015. Measurement of the cooling efficiency of pavement-watering as an urban heat island mitigation technique. J. Sustain. Deve. Energy Water Environ. Syst. 3 (1), 1–11. https://doi.org/10.13044/j.sdewes.2015.03.0001.
Herb, W.R., Janke, B., Mohseni, O., Stefan, H.G., 2008. Thermal pollution of streams by runoff from paved surfaces. Hydrol. Process. 22 (7), 987–999. https://doi.org/10.1002/hyp.6986.
Hirsch, R.M., De Cicco, L.A., 2015. User guide to exploration and graphics for RivEr trends (EGRET) and dataRetrieval: R packages for hydrologic data. U.S. Geological Survey Techniques and Methods Book 4, p. 93.
Hopkins, K.G., Morse, N.B., Bain, D.J., Bettez, N.D., Grimm, N.B., Morse, J.L., ... Suchy, A.K., 2015. Assessment of Regional Variation in streamflow Responses to Urbanization and the Persistence of Physiography. Environmental Science & Technology 49 (5), 2724–2732. https://doi.org/10.1021/es505389y.
Hosen, J.D., McDonough, O.T., Febria, C.M., Palmer, M.A., 2014. Dissolved organic matter quality and bioavailability changes across an urbanization gradient in headwater streams. Environ. Sci. Technol. 48 (14), 7817–7824. https://doi.org/10.1021/es501422z.
Hsieh, J.L., Nguyen, T.Q., Matte, T., Ito, K., 2015. Drinking water turbidity and emergency department visits for gastrointestinal illness in New York City, 2002–2009. PLoS One 10 (4), e0125071. https://doi.org/10.1371/journal.pone.0125071.
Hu, C., Muller-Karger, F.E., Zepp, R.G., 2002. Absorbance, absorption coefficient, and apparent quantum yield: a comment on common ambiguity in the use of these optical concepts. Limnol. Oceanogr. 47 (4), 1261–1267. https://doi.org/10.4319/lo.2002.47.4.1261.
Huey, G.M., Meyer, M.L., 2010. Turbidity as an indicator of water quality in diverse watersheds of the Upper Pecos River basin. Water 2 (2), 273–284. https://doi.org/10.3390/w2020273.
Inserillo, E.A., Green, M.B., Shanley, J.B., Boyer, J.N., 2017. Comparing catchment hydrologic response to a regional storm using specific conductivity sensors. Hydrol. Process. 31 (5), 1074–1085. https://doi.org/10.1002/hyp.11091.
Jefferson, A.J., Bhaskar, A.S., Hopkins, K.G., Fanelli, R., Avellaneda, P.M., McMillan, S.K., 2017. Stormwater management network effectiveness and implications for urban watershed function: a critical review. Hydrol. Process. 31 (23), 4056–4080. https://doi.org/10.1002/hyp.11347.
Jensen, L.R., Davis, J.C., Davis, G.A., 2014. Ketchikan Creeks: Stormwater Quality Assessment. Aquatic Restoration and Research Institute, pp. 1–66.
Jofre, J., Blanch, A.R., Lucena, F., 2010. Water-borne infectious disease outbreaks associated with water scarcity and rainfall events. In: Sabater, S., Barceló, D. (Eds.), Water Scarcity in the Mediterranean: Perspectives Under Global Change, pp. 147–159. https://doi.org/10.1007/698_2009_22.
Kaushal, S.S., Gold, A.J., Bernal, S., Johnson, T.A.N., Addy, K., Burgin, A., ... Belt, K.T., 2018. Watershed 'chemical cocktails': Forming novel elemental combinations in Anthropocene fresh waters. Biogeochemistry 141 (3), 281–305. https://doi.org/10.1007/s10533-018-0502-6.
Kerkez, B., Gruden, C., Lewis, M., Montestruque, L., Quigley, M., Wong, B., Bedig, A., Kertesz, R., Braun, T., Cadwalader, O., Poresky, A., Pak, C., 2016. Smarter stormwater systems. Environ. Sci. Technol. 50 (14), 7267–7273. https://doi.org/10.1021/acs.est.5b05870.
Khandewal, A, González-Pinzón, R, Regier, P, Nichols, J, Van Horn, D, 2020. Introducing the Self-Cleaning FiLtrAtion for Water quaLity SenSors (SC-FLAWLeSS) system. Limnology and Oceanography: Methods Submitted for publication.
Kingsford, R. (Ed.), 2006. Ecology of Desert Rivers, 1st edition Cambridge University Press, New York.
Klaus, J., McDonnell, J.J., 2013. Hydrograph separation using stable isotopes: review and evaluation. J. Hydrol. 505, 47–64. https://doi.org/10.1016/j.jhydrol.2013.09.006.
Kowalczuk, P., Zabłocka, M., Sagan, S., Kuliński, K., 2010. Fluorescence measured in situ as a proxy of CDOM absorption and DOC concentration in the Baltic Sea. Oceanologia 52 (3), 431–471.
Lee, J.H., Bang, K.W., 2000. Characterization of urban stormwater runoff. Water Res. 34 (6), 1773–1780. https://doi.org/10.1016/S0043-1354(99)00325-5.
Li, D., Wan, J., Ma, Y., Wang, Y., Huang, M., Chen, Y., 2015. Stormwater runoff pollutant loading distributions and their correlation with rainfall and catchment characteristics in a rapidly industrialized city. PLoS One 10 (3). https://doi.org/10.1371/journal.pone.0118776.
Lintern, A., Webb, J.A., Ryu, D., Liu, S., Bende-Michl, U., Waters, D., ... Western, A.W., 2018. Key factors influencing differences in stream water quality across space. Wiley Interdisciplinary Reviews: Water 5 (1), e1260. https://doi.org/10.1002/wat2.1260.
Long, D.T., Voice, T.C., Xagoraraki, I., Chen, A., Wu, H., Lee, E., ... Xing, F., 2017. Patterns of c-q hysteresis loops and within an integrative pollutograph for selected inorganic and organic solutes and E. coli in an urban salted watershed during winter-early spring periods. Applied Geochemistry 83, 93–107. https://doi.org/10.1016/j.apgeochem.2017.03.002.
Lozano-Parra, J., Pulido, M., Lozano-Fondón, C., Schnabel, S., 2018. How do soil moisture and vegetation covers influence soil temperature in drylands of Mediterranean regions? Water 10 (12), 1747. https://doi.org/10.3390/w10121747.
Magaud, H., Migeon, B., Morfin, P., Garric, J., Vindimian, E., 1997. Modelling fish mortality due to urban storm run-off: Interacting effects of hypoxia and un-ionized ammonia. Water Res. 31 (2), 211–218. https://doi.org/10.1016/S0043-1354(96)00255-2.
Mallin, M.A., Johnson, V.L., Ensign, S.H., MacPherson, T.A., 2006. Factors contributing to hypoxia in rivers, lakes, and streams. Limnol. Oceanogr. 51 (1part2), 690–701. https://doi.org/10.4319/lo.2006.51.1_part_2.0690.
Mallin, M.A., Johnson, V.L., Ensign, S.H., 2009. Comparative impacts of stormwater runoff on water quality of an urban, a suburban, and a rural stream. Environ. Monit. Assess. 159 (1–4), 475–491. https://doi.org/10.1007/s10661-008-0644-4.
Matson, E.A., Hornor, S.G., Buck, J.D., 1978. Pollution indicators and other microorganisms in river sediment. J. Water Pollut. Control Fed. 50 (1), 13–19.
McGrane, S.J., Hutchins, M.G., Miller, J.D., Bussi, G., Kjeldsen, T.R., Loewenthal, M., 2017. During a winter of storms in a small UK catchment, hydrology and water quality responses follow a clear rural-urban gradient. J. Hydrol. 545, 463–477. https://doi.org/10.1016/j.jhydrol.2016.12.037.
McKenna, O.P., Sala, O.E., 2016. Biophysical controls over concentration and depth distribution of soil organic carbon and nitrogen in desert playas. J. Geophys. Res. Biogeosci. 121 (12), 3019–3029. https://doi.org/10.1002/2016JG003545.
Melcher, A.A., Horsburgh, J.S., 2017. An urban observatory for quantifying phosphorus and suspended solid loads in combined natural and stormwater conveyances. Environ. Monit. Assess. 189 (6), 285. https://doi.org/10.1007/s10661-017-5974-7.
Métadier, M., Bertrand-Krajewski, J.-L., 2012. The use of long-term on-line turbidity measurements for the calculation of urban stormwater pollutant concentrations, loads, pollutographs and intra-event fluxes. Water Res. 46 (20), 6836–6856. https://doi.org/10.1016/j.watres.2011.12.030.
Mihalevich, B.A., Horsburgh, J.S., Melcher, A.A., 2017. High-frequency measurements reveal spatial and temporal patterns of dissolved organic matter in an urban water conveyance. Environ. Monit. Assess. 189 (11), 593. https://doi.org/10.1007/s10661-017-6310-y.
Miller, J.D., Hess, T., 2017. Urbanisation impacts on storm runoff along a rural-urban gradient. J. Hydrol. 552, 474–489. https://doi.org/10.1016/j.jhydrol.2017.06.025.
Miskewitz, Robert, Uchrin, Christopher, 2013. In-stream dissolved oxygen impacts and sediment oxygen demand resulting from combined sewer overflow discharges. J. Environ. Eng. 139 (10), 1307–1313. https://doi.org/10.1061/(ASCE)EE.1943-7870.0000739.
Nelson, K.C., Palmer, M.A., 2007. Stream temperature surges under urbanization and climate change: data, models, and responses1. J. Am. Water Resour. As. 43 (2), 440–452. https://doi.org/10.1111/j.1752-1688.2007.00034.x.
Newcomer, T.A., Kaushal, S.S., Mayer, P.M., Shields, A.R., Canuel, E.A., Groffman, P.M., Gold, A.J., 2012. Influence of natural and novel organic carbon sources on denitrification in forest, degraded urban, and restored streams. Ecol. Monogr. 82 (4), 449–466. https://doi.org/10.1890/12-0458.1.
Ortiz-Hernandez, J., Lucho-Constantino, C., Lizarraga-Mendiola, L., Icela Beltran-Hernandez, R., Coronel-Olivares, C., Vazquez-Rodriguez, G., 2016. Quality of urban runoff in wet and dry seasons: a case study in a semi-arid zone. Environ. Sci. Pollut. Res. 23 (24), 25156–25168. https://doi.org/10.1007/s11356-016-7547-7.
Pellerin, B., Stauffer, B.A., Young, D.A., Sullivan, D.J., Bricker, S.B., Walbridge, M.R., Clyde, G.A., Shaw, D.M., 2016. Emerging tools for continuous nutrient monitoring networks: Sensors advancing science and water resources protection. J. Am. Water Resour. As. 52 (4), 993–1008. https://doi.org/10.1111/1752-1688.12386.
Peters, N.E., 2009. Effects of urbanization on stream water quality in the city of Atlanta, Georgia, USA. Hydrol. Process. 23 (20), 2860–2878. https://doi.org/10.1002/hyp.7373.
Peters, D.P.C., Gibbens, R.P., 2006. Plant communities in the jordana basin: the dynamic landscape. Structure and Function of a Chihuahuan Desert Ecosystem: The Jornada

Basin Long-Term Ecological Research Site. Oxford University Press, Oxford, U.K, pp. 211–231.
Pilon, B.S., Tyner, J.S., Yoder, D.C., Buchanan, J.R., 2019. The effect of pervious concrete on water quality parameters: a case study. Water 11 (2), 263. https://doi.org/10.3390/w11020263.
R Core Team, 2018. A Language and Environment for Statistical Computing. R Foundation for Statistical Computing, Vienna, Austria https://www.R-project.org/.
Raymond, P.A., Saiers, J.E., 2010. Event controlled DOC export from forested watersheds. Biogeochemistry 100 (1), 197–209. https://doi.org/10.1007/s10533-010-9416-7.
Reale, J.K., Van Horn, D.J., Condon, K.E., Dahm, C.N., 2015. The effects of catastrophic wildfire on water quality along a river continuum. Freshw. Sci. 34 (4), 1426–1442. https://doi.org/10.1086/684001.
Regier, P., Jaffé, R., 2016. Short-term dissolved organic carbon dynamics reflect tidal, water management, and precipitation patterns in a subtropical estuary. Front. Mar. Sci. 3. https://doi.org/10.3389/fmars.2016.00250.
Rehg, K.J., Packman, A.I., Ren, J., 2005. Effects of suspended sediment characteristics and bed sediment transport on streambed clogging. Hydrol. Process. 19 (2), 413–427. https://doi.org/10.1002/hyp.5540.
Rice, P.J., Horgan, B.P., Hamlin, J.L., 2018. Off-site transport of fungicides with runoff: a comparison of flutolanil and pentachloronitrobeneze applied to creeping bentgrass managed as a golf course fairway. Ecotoxicol. Environ. Saf. 157, 143–149. https://doi.org/10.1016/j.ecoenv.2018.03.070.
Rivers, E.N., McMillan, S.K., Bell, C.D., Clinton, S.M., 2018. Effects of urban stormwater control measures on denitrification in receiving streams. Water 10 (11), 1582. https://doi.org/10.3390/w10111582.
Rook, J.J., 1977. Chlorination reactions of fulvic acids in natural waters. Environ. Sci. Technol. 11 (5), 478–482. https://doi.org/10.1021/es60128a014.
Salomons, W., Förstner, U., 1984. Metals in the Hydrocycle. https://doi.org/10.1007/978-3-642-69325-0.
Saraceno, J.F., Shanley, J.B., Downing, B.D., Pellerin, B.A., 2017. Clearing the waters: evaluating the need for site-specific field fluorescence corrections based on turbidity measurements. Limnol. Oceanogr. Methods 15 (4), 408–416. https://doi.org/10.1002/lom3.10175.
Schwartz, J., Levin, R., Goldstein, R., 2000. Drinking water turbidity and gastrointestinal illness in the elderly of Philadelphia. J. Epidemiol. Community Health 54 (1), 45–51. https://doi.org/10.1136/jech.54.1.45.
Schwientek, M., Osenbrück, K., Fleischer, M., 2013. Investigating hydrological drivers of nitrate export dynamics in two agricultural catchments in Germany using high-frequency data series. Environ. Earth Sci. 69 (2), 381–393. https://doi.org/10.1007/s12665-013-2322-2.
Sequeria, R., Lung, F., 1995. A critical data analysis and interpretation of the pH, ion loadings and electrical conductivity of rainwater from the territory of Hong Kong. Atmos. Environ. 29 (18), 2439–2447. https://doi.org/10.1016/1352-2310(95)00161-Q.
Shephard, Z.M., Conn, K.E., Beisner, K.R., Jornigan, A.D., Bryant, C.F., 2019. Characterization and Load Estimation of Polychlorinated Biphenyls (PCBs) From Selected Rio Grande Tributary Stormwater Channels in the Albuquerque Urbanized Area, New Mexico, 2017–18. (Report No. 2019–1106; p. 61). https://doi.org/10.3133/ofr20191106.
Sheppard, P.R., Comrie, A.C., Packin, G.D., Angersbach, K., Hughes, M.K., 2002. The climate of the US Southwest. Clim. Res. 21 (3), 219–238. https://doi.org/10.3354/cr021219.
Somers, K.A., Bernhardt, E.S., Grace, J.B., Hassett, B.A., Sudduth, E.B., Wang, S., Urban, D.L., 2013. Streams in the urban heat island: spatial and temporal variability in temperature. Freshw. Sci. 32 (1), 309326. https://doi.org/10.1899/12-046.1.
Stroud Water Research Center, 2020. Model My Watershed [Software]. Available from. https://wikiwatershed.org/.
Storms, E.F., Oelsner, G.P., Locke, E.A., Stevens, M.R., Romero, O.C., 2015. Summary of urban stormwater quality in Albuquerque, New Mexico, 2003–12. U.S. Geological Survey Scientific Investigations Report 2015–5006 Available online at http://dx.doi.org/10.3133/sir20155006.
Summers, B., 2019. Multi-Year Water Quality Data Reveal Highly Variable Timing and Magnitude of Metabolism and Physicochemical Drivers in an Aridland River Network. Dissertation. University of New Mexico Retrieved from. https://digitalrepository.unm.edu/ce_etds/241/.
Thompson, A.M., Kim, K., Vandermuss, A.J., 2008. Thermal characteristics of stormwater runoff from asphalt and sod surfaces1. J. Am. Water Resour. As. 44 (5), 1325–1336. https://doi.org/10.1111/j.1752-1688.2008.00226.x.
Tuszynski, J., 2019. CaTools: Tools: Moving Window Statistics, GIF, Base64, ROC AUC, etc (Version 1.17.1.2).
USFWS, 2011. Biological Opinion on the Albuquerque MS4 Stormwater Permit. U.S Fish and Wildlife Service, New Mexico Ecological Services Office, Albuquerque, New Mexico https://www.fws.gov/southwest/es/NewMexico/documents/BO/2011-F-0024_AMAFCA_ABQ_MS4_Permit.pdf.
Vivoni, E.R., Bowman, R.S., Wyckoff, R.L., Jakubowski, R.T., Richards, K.E., 2006. Analysis of a monsoon flood event in an ephemeral tributary and its downstream hydrologic effects. Water Resour. Res. 42 (3). https://doi.org/10.1029/2005WR004036.
Wagner, R.J., Boulger, R.W.J., Oblinger, C.J., Smith, B.A., 2006. Guidelines and standard procedures for continuous water-quality monitors: station operation, record computation, and data reporting. United States Geological Survey Techniques and Methods 1-D3.
Walsh, C.J., Roy, A.H., Feminella, J.W., Cottingham, P.D., Groffman, P.M., Morgan, R.P., 2005. The urban stream syndrome: current knowledge and the search for a cure. Freshw. Sci. 24 (3), 706–723. https://doi.org/10.1899/04-028.1.
Wasserstein, R.L., Schirm, A.L., Lazar, N.A., 2019. Moving to a world beyond "$p < 0.05$". Am. Stat. 73 (sup1), 1–19. https://doi.org/10.1080/00031305.2019.1583913.
Watras, C.J., Hanson, P.C., Stacy, T.L., Morrison, K.M., Mather, J., Hu, Y.-H., Milewski, P., 2011. A temperature compensation method for CDOM fluorescence sensors in freshwater. Limnol. Oceanogr. Methods 9 (7), 296–301. https://doi.org/10.4319/lom.2011.9.296.
Wenger, S.J., Roy, A.H., Jackson, C.R., Bernhardt, E.S., Carter, T.L., Filoso, S., ... Walsh, C.J., 2009. Twenty-six key research questions in urban stream ecology: An assessment of the state of the science. Journal of the North American Benthological Society 28 (4), 1080–1098. https://doi.org/10.1899/08-186.1.
Wengrove, M.E., Ballestero, T.P., 2012. Upstream to downstream: stormwater quality in Mayagüez, Puerto Rico. Environ. Monit. Assess. 184 (8), 5025–5034. https://doi.org/10.1007/s10661-011-2318-x.
Wicke, D., Cochrane, T.A., O'Sullivan, A.D., Cave, S., Derksen, M., 2014. Effect of age and rainfall pH on contaminant yields from metal roofs. Water Sci. Technol. 69 (10), 2166–2173. https://doi.org/10.2166/wst.2014.124.
Wickham, H., 2016. ggplot2: Elegant Graphics for Data Analysis.
Wise, J.L., Van Horn, D.J., Diefendorf, A.F., Regier, P.J., Lowell, T.V., Dahm, C.N., 2019. Dissolved organic matter dynamics in storm water runoff in a dryland urban region. J. Arid Environ. https://doi.org/10.1016/j.jaridenv.2019.03.003.
Yang, Y.-Y., Toor, G.S., 2018. Stormwater runoff driven phosphorus transport in an urban residential catchment: implications for protecting water quality in urban watersheds. Sci. Rep. 8 (1), 1–10. https://doi.org/10.1038/s41598-018-29857-x.
Young, P.C., 2006. Rainfall-runoff modeling: transfer function models. Encyclopedia of Hydrological Sciences. https://doi.org/10.1002/0470848944.hsa141a.
Young, P.C., Taylor, J.C., Tych, W., Pedregal, D.J., McKenna, P.G., 2010. The Captain Toolbox. Software. Lancaster University, Lancaster Retrieved from. http://wp.lancs.ac.uk/captaintoolbox/.
Zeiger, S.J., Hubbart, J.A., 2018. Quantifying land use influences on event-based flow frequency, timing, magnitude, and rate of change in an urbanizing watershed of the central USA. Environ. Earth Sci. 77 (3), 107. https://doi.org/10.1007/s12665-018-7312-y.